applied sciences

MDPI

Article

Software for Monitoring the In-Service Efficiency of Hydraulic Pumps

Alin-Adrian Anton [1,*], Adrian Cococeanu [2] and Sebastian Muntean [3,*]

[1] Computer and Information Technology Deparment, Faculty of Automation and Computing, Politehnica University Timişoara, 2nd Vasile Pârvan Ave., 300223 Timişoara, Romania
[2] AQUATIM S.A. Timişoara, 11/A Gheorghe Lazăr Str., 300081 Timişoara, Romania
[3] Center for Fundamental and Advanced Technical Research, Romanian Academy Timişoara Branch, 24th Mihai Viteazu Ave., 300222 Timişoara, Romania
* Correspondence: alin.anton@upt.ro (A.-A.A.); sebastian.muntean@academiatm.ro (S.M.)

Abstract: The present paper introduces the creation of an algorithm and the software used to determine the energetic performance and monitor the efficiency of hydraulic pumps working in various industrial applications, such as water supply systems, water treatment processes, and irrigation systems, particularly in the cases where there is no permanent monitoring. Our field investigations and the surveyed literature show that the only parameter that is neither monitored nor computed is the efficiency of the pumps. The software implementation allows for determining the in-service efficiency of the pumps and comparing it to the value associated with the best efficiency point (BEP). The solution is user-friendly and can be easily installed on any computer or smartphone. The software has been applied and tested in the Hydraulic Machines Laboratory at the "Politehnica" University Timişoara and at the AQUATIM S.A. regional water supply company. The software module monitors the operating regimes of the pumps and supports the deployment of predictive maintenance and servicing.

Keywords: cellular phones; energy consumption; hydraulic pumps; software algorithm; water resources

Citation: Anton, A.-A.; Cococeanu, A.; Muntean, S. Software for Monitoring the In-Service Efficiency of Hydraulic Pumps. *Appl. Sci.* **2022**, *12*, 11450. https://doi.org/10.3390/app122211450

Academic Editors: Vasily Novozhilov and Cunlu Zhao

Received: 13 October 2022
Accepted: 8 November 2022
Published: 11 November 2022

1. Introduction

Water and energy are two vital sources of any urban community's daily life. In the United States, 19% of all the energy produced is consumed for the supply of drinking water, including treatment, transportation, storage, distribution, collecting of sewage water, treatment and discharge [1].

The situation is almost the same in the European Union, where 22% of the total electricity consumption of the industrial systems fitted with electric engines runs the pumps; the annual electricity consumption was 109 TWh in 2005 for water pumping, and in 2020, the increase in energy consumption was 136 TWh, a growth of 25% [2].

The life cycle cost of centrifugal pumps installed in industrial applications consists mainly of maintenance and energy costs. The energy cost is the most significant contribution in the total life cycle cost of a pump [3,4]. Depending on the industry in which the centrifugal pumps are installed, the total life-cycle cost comes from the consumption of electric power (e.g., chemical industry 26%, pulp and paper 31%, petroleum 59%, water treatment and supply systems from 55% to 90%) [5].

Proper selection of the pump in correlation with the system requirements can reduce energy costs by an average of 20%. This means that the pump operates mostly with maximum efficiency in the vicinity of the best efficiency point (BEP). In contrast, the hydraulic pumps that operate at off-design conditions lead to premature damage, wasted costs and

costly repairs or replacements [6]. All these issues can be avoided by selecting the appropriate pump, monitoring it and providing well-planned maintenance [7]. This applies to all situations involving the operation of pumps and particularly in cases where an adequate monitoring system is missing.

Once the pump is installed, its efficiency is determined by the process conditions. The major factors affecting performance include the efficiency of the pump and system components, overall system design, efficient pump control and appropriate maintenance cycles. To achieve the efficiencies available from the mechanical design, pump manufacturers must work closely with end users and design engineers to consider all of these factors when specifying pumps [8].

The only parameters that are neither determined nor examined are the pump and pumping station efficiencies, although all the other variables (absorbed power, pumping head) are measured to determine and calculate these parameters.

Energy savings represent lower operating costs and higher performance. The most obvious energy savings are those associated with improvements in pump efficiency [9]. Although worth pursuing, they are small compared to the efficiency gains that can be achieved through a proper analysis of the pumping system to obtain the best fit of the pump to the system and the operating requirements. It may be comforting to select the nominal flow rate (at the highest value of the flow rate). However, the energy penalty can be significant when the pump is operating at partial flow rates.

A correctly selected maximum flow rate is a key value where energy optimization is targeted. Most pumps run far from their BEP. For reasons ranging from short-sighted or overly conservative design, specification and procurement to decades of incremental changes in operating conditions, pipes and control valves are too large or too small. In anticipation of future load growth, the end user, supplier and design engineers routinely add 10–50% safety margins to ensure the pump and motor can accommodate anticipated capacity increases. Important energy savings can be made if the safety margins imposed to obtain the rated service condition are not excessive [3].

The average pumping accounted for 80% of total electricity use in public water systems, as reported by EPRI [5]. The use of electricity for water and wastewater treatment has grown during the last 20 years and will continue to grow. The efficiency of the pump affects the pumping performance significantly. The efficiency of pumping units is often relatively low because pumps are typically oversized [10].

The relative significance of different energy-using systems will vary depending on the system, yet a "typical" treatment system can be developed and presented. The distribution of energy within the water treatment conveyance, treatment, and distribution cycle of a surface water system shows one approach based on certain key assumptions. The data do not apply to all water treatment systems but instead provide context as to the energy issues within water treatment facilities. In this case, pumping sewage accounts for 67%, water treatment for 14%, raw water pumping for 11%, and in-plant water pumping for 8% [1] of total energy use.

In addition to the energy costs, inefficient operation of the pump units could impact system reliability because the mechanical reliability of a pumping unit is linked to the pump efficiency, and any damage to a pump unit may entail substantial additional costs. Consequently, efficient pump operation over the lifespan of a system is a key element of any cost-reduction program.

In general, adjusting the flow rate using the variable speed drive (VSD) of centrifugal pumps is efficient. When a VSD does not exist, the pump's duty point can be tuned using the valve installed on the pump discharge line or by modifying the number of operating pumps. These pump-tuning methods are frequently selected but are inefficient, leading to the adjustment of the flow rate through hydraulic losses. The surveyed literature underlines that studies of and patents for the monitoring of pump operating parameters exist, mostly oriented towards the determination of the pumped flow rate and the pumping head [11] by measuring the parameters of the electric motor that drives the pump. There are also

concerns noted in studies and research about the reduction in the pumps' efficiency in their duty point [12–18]. The only parameter that is not measured, computed or informatively shown is the pump efficiency and the pumping station efficiency. Researchers state that the pump efficiency can be determined, but they do not provide a methodology or a solution to do so.

At the same time, it is rather simple to measure the pressure, the flow rate and various electric parameters, regardless of the operating mode of the pumping stations (manual or automated), to particularize the operation of the pumps and the pumping unit and optimize the system in service.

The paper presents the software solution developed for monitoring hydraulic pumps installed in pumping stations. The software identifies the pump's operating regime by determining the efficiency at the duty point and fitting this value within the boundaries set by the operator.

To begin, one must know the efficiency behavior of the pump from the catalog or laboratory investigations. Efficiency can also be determined in situ using various indirect methods [15–18] and subsequent calculations or direct methods, such as the thermodynamic method, which can be used in the case of large-capacity pumps [19,20].

A pump's energetic behavior (efficiency curves) can be determined based on the manufacturer's catalog data or data obtained from previous tests [21]. The main geometric parameters can be determined in situ. All the geometric parameters and the coefficients of the longitudinal and local hydraulic losses are inserted in a visible barcode for each pump. After scanning the barcode with a smartphone, the operator inputs two parameters, p_s—suction pressure and p_d—discharge pressure, available on the two manometers already installed on the pumps. The software identifies the duty point of the pump and establishes the operating regime, comparing the value of the efficiency at the duty point to the maximum efficiency of the pump. Finally, the software issues a recommendation to the operator about its normal/abnormal operation and suggests to the operator how to act [22].

The pumps installed in different systems need to be operated safely at a low cost. Monitoring and preventive maintenance of centrifugal pumps are crucial issues to increase their reliability and diminish the costs [23,24]. Industry 4.0 principles must be implemented in drinking water systems to provide an efficient link between the pumping units and monitoring systems so the operator can make the best decisions [25]. The software module presented in this manuscript is a basic component of this system.

Our field investigations and the surveyed literature show that the only parameter that is neither monitored nor computed is the efficiency of the pumps. Even though the power factor and the efficiency of the electric motors are provided by their manufacturers, Ferreira et al. [26] conducted extensive tests on 435 three-phase induction electric motors from 38 different manufacturers between 2015 and 2016, showing that 58% of the values measured for the power factor of the motors were lower than those reported by the manufacturer [26], and also that 55% of the measured values for the performance were lower than the values reported by the manufacturer [26]. The pump efficiency value **is ignored in practice** and many industry studies such as [7] prove that improper design and poor pump performance may affect the plant operation such as maintenance cost, downtime and loss of production. Consequently, the software implementation allows for determining the in-service efficiency of the pumps and comparing it to the value associated with the best efficiency point (BEP).

The development of a robust algorithm to assess hydraulic pump efficiency is detailed in Section 2. Free software packages have been selected to implement the algorithm, ensuring its portability on any operating system. The implementation of the algorithm and the selected software packages is detailed in Section 3. Within Section 4 the application of the software module in the operating of the PCN 65/200 centrifugal pump installed in the laboratory is discussed, which allows the determination of percentage deviations of the results supplied for the full range of operation. Section 4.1 contains the available data for

the PCN 65/200 centrifugal pump that have been used for the sensitivity analysis of the algorithm regarding the input values and the parameters associated with the investigated hydraulic configuration for various operating points, covering the full operating range of the pump. The sensitivity analysis allows determining the influence of the input values and the parameters associated with the hydraulic configuration over the output values of the algorithm and their ranking according to the level of percentage deviation. The results obtained with the software module implemented in the regional water supply company, AQUATIM S.A., for the monitoring of the in situ operation of the Worthington 500 LNN-775A double flux pumps of 1 MW, ensuring the water supply of Timişoara city, are shown in Section 5. The conclusions regarding the development and testing of the software module to monitor hydraulic pump efficiency are summarized in Section 6.

2. Algorithm for Assessing Pump Efficiency

A robust algorithm is developed to monitor the efficiency of in-service pumps. The η_P pump efficiency equation is:

$$\eta_P = \frac{P_h}{P_m} = \frac{g\rho QH}{P_m} \quad (1)$$

where $P_h = g\rho QH$ [W] is the hydraulic power, representing the power transferred to the liquid, Q [m^3/s] is the pump discharge (volumetric flow rate), H [m] represents the pumping head, ρ [kg/m^3] is the density of the working liquid (water), g [m/s^2] is the gravity acceleration, and P_m [W] represents the mechanical power at the pump shaft.

The pumping head H is presented in Equation (2).

$$H = \frac{(p_d - p_s)}{g\rho} + \frac{8Q^2}{g\pi^2}\left[\frac{1}{D_d^4} - \frac{1}{D_s^4}\right] + (z_d - z_s) \quad (2)$$

This equation is valid if the instruments are installed on the pump flanges. In practical terms, the instruments cannot be installed on the pump flanges in most cases. That is why the algorithm will be considered with a generalized form of the equation of the pumping head H given in Equation (3). This equation includes the distributed and local hydraulic losses due to the positioning of the instruments in relationship to the pump flanges and the static pressures measured on the suction and discharge lines.

$$H = \frac{(p_d - p_s)}{g\rho} + \frac{8Q^2}{g\pi^2}\left[\frac{1}{D_d^4}\left(\lambda_d \frac{l_d}{D_d} + \zeta_d + 1\right) + \frac{1}{D_s^4}\left(\lambda_s \frac{l_s}{D_s} + \zeta_s - 1\right)\right] + (z_d - z_s) \quad (3)$$

where p_s and p_d are the static pressures measured at the pump's suction and discharge, l_s, D_s, λ_s, ζ_s are the length, diameter, coefficient of distributed hydraulic loss, or Darcy's coefficient, and the local hydraulic loss coefficient, in connection with the position of the instrument installed on the suction line compared to the pump flange, l_d, D_d, λ_d, ζ_d are the length, diameter, coefficient of distributed hydraulic loss, or the Darcy's coefficient and the local hydraulic loss coefficient, in connection with the position of the instrument installed on the discharge line compared to the pump flange, and $z_d - z_s$ is the quota difference between the position of the instrument installed on the discharge line and the suction line. The generalized equation of the pumping head (3) is reduced to (2) when the instruments are installed on the pump flanges, because the distributed hydraulic loss coefficients $\lambda_s = \lambda_d = 0$ and the local hydraulic loss coefficients $\zeta_s = \zeta_d = 0$.

It is important to mention that for the present algorithm, we need only the readings of the static suction pressure p_s and discharge pressure p_d to determine the efficiency η_P of the pump. The remaining values needed for the calculus are **determined** (e.g., the volumetric flow rate that has passed through the pump Q—a value difficult to determine in industrial applications), or **assessed** (the mechanical power by the pump P_m).

The pumping head is defined as the specific energy difference of the fluid between the inlet section and the outlet section of the pump. The pumping head is given by the $H(Q)$ curve from the pump supplier's catalog or by the measurements performed in situ. As a

result, the $H(Q)$ curve can be expressed in the form of a 2nd-degree polynomial for a radial centrifugal pump. The coefficients h_2, h_1 and h_0 are determined by a fitting procedure using the available data.

$$H(Q) = h_2Q^2 + h_1Q + h_0 \tag{4}$$

The algorithm for assessing the efficiency of hydraulic pumps is based on knowing the pump's catalog features (or the pump's curves, determined experimentally) and the determination of geometric data in situ, which will be introduced as parameters of the algorithm.

The value of the volumetric flow rate Q [m^3/s] is obtained from the equality of the relationships (3) and (4) by solving the 2nd-degree equation below.

$$Q^2\{h_2 - \frac{8}{g\pi^2}[\frac{1}{D_d^4}(\lambda_d\frac{l_d}{D_d} + \zeta_d + 1) + \frac{1}{D_s^4}(\lambda_s\frac{l_s}{D_s} + \zeta_s - 1)]\} + h_1Q + [h_0 - (z_d - z_s - \frac{(p_d - p_s)}{g\rho})] = 0 \tag{5}$$

The 2nd-degree equation for the volumetric flow rate in Equation (5) is written in the following manner:

$$t_2Q^2 + t_1Q + t_0 = 0 \tag{6}$$

for which the following terms have been used:

$$\begin{aligned} t_0 &= h_0 - \Delta z - \frac{(p_d - p_s)}{g\rho} \\ t_1 &= h_1 \\ t_2 &= h_2 - \frac{8}{g\pi^2}[\frac{1}{D_d^4}(\lambda_d\frac{l_d}{D_d} + \zeta_d + 1) + \frac{1}{D_s^4}(\lambda_s\frac{l_s}{D_s} + \zeta_s - 1)] \end{aligned} \tag{7}$$

where Δz is defined by Equation (8):

$$\Delta z = z_d - z_s \tag{8}$$

The solutions of the 2nd-degree polynomial equation presented in Equation (6) for flow rate are:

$$Q_{1,2} = \frac{-t_1 \pm \sqrt{{t_1}^2 - 4t_2t_0}}{2t_2} \tag{9}$$

Of the two solutions of Equation (6), the one with the positive value shall be retained ($Q_1 > 0$).

Once the Q_1 value is known, the coefficients h_2, h_1 and h_0 for the $H(Q)$ curve in Equation (4), the p_3, p_2, p_1 and p_0 coefficients for the $P_m(Q)$ curve in Equation (10), respectively, e_2, e_1 and e_0 coefficients for $\eta_P(Q)$ curve in Equation (11) are used for calculating the pumping head value $H(Q_1)$, the mechanical power value $P_m(Q_1)$ and the pump efficiency $\eta_P(Q_1)$. These coefficients are determined by a fitting procedure, applied to the available data.

$$P_m(Q) = p_3Q^3 + p_2Q^2 + p_1Q + p_0 \tag{10}$$

$$\eta_P(Q) = e_2Q^2 + e_1Q + e_0 \tag{11}$$

The value of the volumetric flow rate corresponding to the BEP is obtained from Equation (12):

$$Q(\eta_{P_{BEP}}) = -\frac{e_1}{2e_2} \tag{12}$$

The value is positive for all the cases $Q(\eta_{P_{BEP}}) > 0$ because the coefficient $e_2 < 0$ is associated with the efficiency curve of η_P pump, which is a vertex-up parabola. The $\eta_{P_{BEP}}$ value is obtained by introducing the value $Q(\eta_{P_{BEP}})$ in Equation (11). This value of the maximum efficiency $\eta_{P_{BEP}}$ corresponding to each constant speed pump is used as

a reference value to define the pump's operating regime. We notice that the maximum efficiency value $\eta_{P_{BEP}}$ of the BEP is determined from the input values and is different for each pump.

The pump's operating regime is determined by comparing the efficiency value η_P of the pump's duty point with the reference value corresponding to the pump's maximum efficiency $\eta_{P_{BEP}}$. Three operating regimes are defined for a hydraulic pump using color vision deficiency codes, containing both text and color flag information as follows:

- Normal operation (NO) from an efficiency point of view (GREEN):

$$0.9\eta_{P_{BEP}} < \eta_P < 1.05\eta_{P_{BEP}}$$

  Normal operation (NO) means the pump is operating at the proper efficiency. That is, the costs of energy consumption for pumping are justified. The operation of the pump in this range will be marked with GREEN ;
- Operation at the limit (LO), from an efficiency point of view: needs scheduled maintenance (YELLOW):

$$0.8\eta_{P_{BEP}} < \eta_P < 0.9\eta_{P_{BEP}} \text{ or}$$
$$1.05\eta_{P_{BEP}} < \eta_P < 1.1\eta_{P_{BEP}}$$

  A pump operating at the limit (LO) suggests the pump is operating with an acceptable efficiency but requires more power than is ideal. A pump operating under these conditions requires scheduled maintenance to identify and address any issues that may have occurred. The operation of the pump under these conditions will be signaled using the color YELLOW ;
- Abnormal operation (AO) from an efficiency point of view: needs urgent maintenance (RED):

$$\eta_P < 0.8\eta_{P_{BEP}} \text{or} \eta_P > 1.1\eta_{P_{BEP}}.$$

  A pump operating under abnormal operation (AO) is pumping with low efficiency and requires additional power to pump. A pump operating under these conditions requires urgent maintenance to identify and address any issues that may have occurred. The operation of the pump under these conditions will be signaled using the color RED .

The green stripe corresponds to Preferred Operating Region (POR) in our selection, while the extreme limits of the yellow area define the Allowable Operating Region (AOR) [4]. To be more explicit, the allowable operating region (AOR) is the operating zone provided by the manufacturer and it includes the yellow zones together with the green zone in our selection.

The reference values predefined by $\eta_{P_{BEP}}$ to circumscribe the fields of operation can be selected by each user based on the pump's operating conditions and on the recommendations issued by its manufacturer. The algorithm allows us to define these reference values for each pump by introducing them into their set of input values. Thus the predefined reference levels can be customized from one pump to another, depending on the required operating conditions and the specific in situ conditions [27] ch. 3.

The boundaries of the operating regions (e.g., POR, AOR) in our algorithm are selected based on the pump efficiency boundaries. The limits of the operating regions defined in other references are related to the volumetric flow rate limits (e.g., range from -30% Q_{BEP} to +15% Q_{BEP} [28,29] range from -10% Q_{BEP} to +10% Q_{BEP} [4] and range from -20% Q_{BEP} to +20% Q_{BEP} reference [30]. We consider that this concept of defining operating region boundaries using pump efficiency is better suited when the pump operation strategy is targeted, rather than defining operating region boundaries by selecting volumetric flow rate.

3. Implementation of an Algorithm to Assess Pump Efficiency

Free software packages that provide portability on any operating system have been selected to implement the software solution. The GNU GSL scientific software library provides robust interpolation, extrapolation and curve-fitting instruments and assessment of the approximation errors [31].

The free package Qt [32] was used to develop the graphic interface. The algorithm's implementation is structured on independent components, materialized by individual processes and tools in the command line, separated from the user interface.

Figure 1 shows the data flow diagram of the software solution.

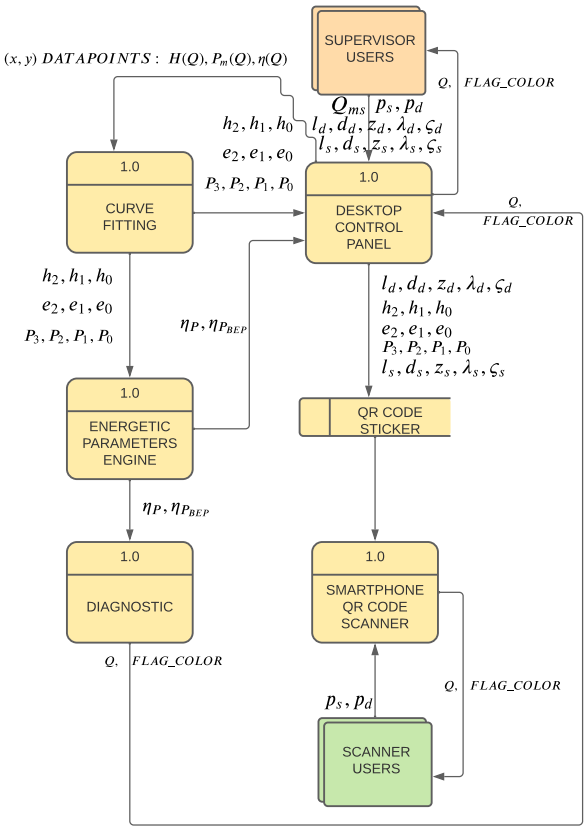

Figure 1. Diagram of the data flow in the software system.

A series of data are read from the additions $H(Q)$, $\eta_P(Q)$ and $P_m(Q)$, made available from the manufacturer's catalog or experimental data. Based on these, the fitting coefficients h_2, h_1, and h_0 are determined for the approximation of the $H(Q)$ curve, which takes its shape from Equation (4). The fitting coefficients e_2, e_1, and e_0 are determined for the approximation of the $\eta(Q)$ curve, which takes its shape from Equation (11), and the fitting coefficients p_3, p_2, p_1 and p_0 are determined for the approximation of the $P_m(Q)$ curve, which takes its shape from Equation (10).

Using these coefficients, the current efficiency value η_P and the maximum efficiency value of the BEP ($\eta_{P_{BEP}}$) are determined, located on the vertex of the efficiency parabola.

The desktop application generates and prints the QR code with the parameters of the hydraulic pathway, l_s, d_s, λ_s, ζ_s l_d, d_d, λ_d, ζ_d. The static pressures measured during suction p_s and discharge p_d lines are input by the user in both smartphone and desktop applications, optionally accompanied by the volumetric flow rate running through the pump Q_{ms}.

The mobile phone application scans the coefficients of the hydraulic pathway from the printed QR code and, based on the measured values of the static suction pressure p_s and those of the discharge p_d computes the efficiency values η_P and $\eta_{P_{BEP}}$ based on which

they can diagnose the operating regime of the pump and return the red, yellow or green code using *FLAG_COLOR*.

Figure 2 shows the diagram of the efficiency assessment algorithm for constant speed hydraulic pumps—Algorithm 1.

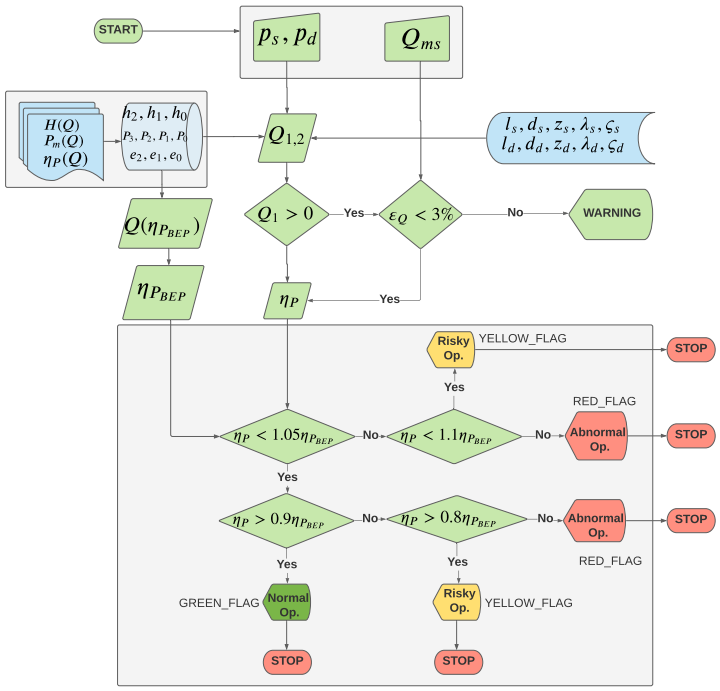

Figure 2. Diagram of the assessment algorithm for hydraulic pump efficiency while operating at constant speed.

Algorithm 1 The assessment algorithm for hydraulic pump efficiency while operating at constant speed

$HQ[] \leftarrow read(HQ)$ ▷ $H(Q)$ data points
$EQ[] \leftarrow read(EQ)$ ▷ $\eta(Q)$ data points
$PQ[] \leftarrow read(PQ)$ ▷ $P_m(Q)$ data points
$h[] \leftarrow fit(HQ)$ ▷ get 2nd order polynomial coefficients
$e[] \leftarrow fit(EQ)$ ▷ get 2nd order polynomial coefficients
$P[] \leftarrow fit(PQ)$ ▷ get 3rd order polynomial coefficients
procedure DIAGNOSTIC(p_s, p_d, Q_{ms})
    $\eta_P, \eta_{P_{BEP}} \leftarrow \eta(h, e, P)$
    if $(\eta_P < 1.05\eta_{P_{BEP}})$ **then**
        if $(\eta_P > 0.9\eta_{P_{BEP}})$ **then**
            $FLAG\_COLOR \leftarrow GREEN$
        else if $(\eta_P > 0.8\eta_{P_{BEP}})$ **then**
            $FLAG\_COLOR \leftarrow YELLOW$
        else
            $FLAG\_COLOR \leftarrow RED$
        end if
    else if $(\eta_P < 1.1\eta_{P_{BEP}})$ **then**
        $FLAG\_COLOR \leftarrow YELLOW$
    else
        $FLAG\_COLOR \leftarrow RED$
    end if
end procedure

Using the reading and data fitting component in Figure 2 for a finite set of data received as input for $H(Q)$, $P_m(Q)$, respectively, $\eta_P(Q)$, the best 2nd- and 3rd-order polynomial functions are obtained and, automatically, the values for these curves' coefficients, with a minimal square error:

$$\chi^2 = (\sum_{i}^{w_i} y_i - \sum_{j}^{x_{ij}} c_j)^2 = ||y - X_c||_{w^2} \tag{13}$$

where y is the input data vector of order n, X is a $n\ x\ p$ matrix having predictor variables, and c is the vector with those p fitting coefficients that must be estimated. The matrix $w = diag(w_1 w_2 \dots w_n)$ contains the weights of the observed vector. The χ^2 square error also takes the form in Equation (17) where $w_i = (y_i - f(x_i))^{-2}$.

The determination of the values of the polynomial curve coefficients has been performed using the GSL Scientific Software Library [31] available as free software and tested in numerous scientific and engineering applications on the market.

The measured volumetric flow rate passing through the pump, Q_{ms}, is used to verify the percentage error ε_Q compared to the value estimated by the algorithm. The user receives a warning if the error exceeds the 3% threshold. The flowmeters used by the water supply company have an accuracy limit of $\pm 3\%$.

Figure 3 shows a diagram of the application's use cases. The operator uses a mobile phone to enter the suction and discharge pressure values, p_s and p_d, and then scans the QR barcode with the parameters configured and printed in the desktop application. Optionally, this software application can also be used to assess the percentage error ε_Q if the measured volumetric flow rate value Q_{ms} is available as input data; see Figure 2.

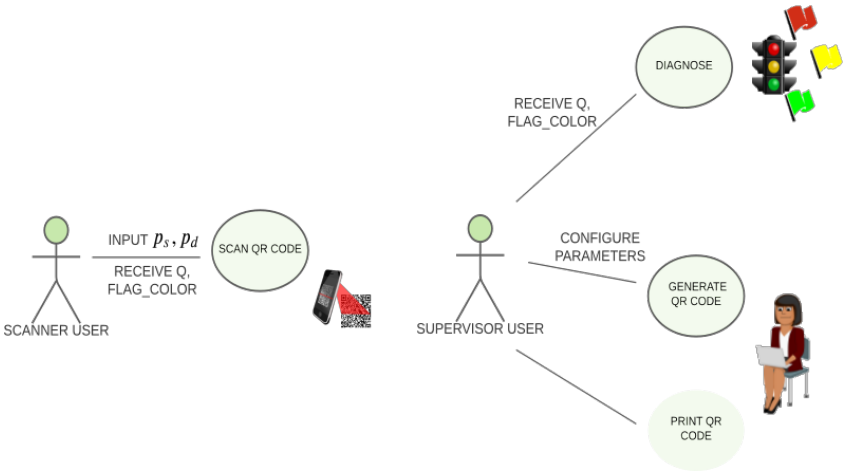

Figure 3. Use case diagram for the software solution.

After reading the barcode that identifies each pump, containing its hydraulic configuration, and after the input of the two read data, p_s and p_d, the duty point of the hydraulic pump is determined. Then, the pump efficiency of the duty point is compared with the BEP value. The hydraulic pump operates normally if the duty point falls in the green region. The pump operation is defective if the duty point falls into the other regions, and the operator must look for the causes and determine the appropriate intervention.

The R^2 parameter will be used to approximate the set of points with the selected polynomial function, defined as follows:

$$R^2 = 1 - \frac{\chi^2}{TSS} \tag{14}$$

where

$$TSS = \sum_{i}^{n} (x_i - \bar{x})^2 \tag{15}$$

is the total sum of the squares of the variations compared to the average value

$$\bar{x} = \frac{1}{n}\sum_{i}^{n} ix_i \tag{16}$$

and

$$\chi^2 = \sum_{i}^{n}(y_i - f(x_i))^2 \tag{17}$$

is determined with the approximation function for those n experimental read data.

The approximation of the set of points n with the selected polynomial function is more precise when the R^2 parameter is closer to 1. Moreover, $R^2 < 1$ as long as $n + 1 < N$ where n is the approximation polynomial's order, and N is the total number of read data values in the input set.

4. The Laboratory Validation of the Software Module for the Pump's Full Operating Range

The algorithm provides the values of the computed variables Q, H, P_m and η_P of the pump's operating point. Moreover, the following values are found as output data: $Q(\eta_{P_{BEP}})$, $H(\eta_{P_{BEP}})$ and $P(\eta_{P_{BEP}})$, and the 10 coefficients of the polynomial functions that approximate the input data for the pump: three coefficients (h_2, h_1 and h_0) for the $H(Q)$ curve, four coefficients (p_3, p_2, p_1 and p_0) for the $P_m(Q)$ curve, three coefficients (e_2, e_1 and e_0) for the $\eta_P(Q)$ curve, and, finally, those three R^2 coefficients that allow for accurate estimation of the read data. In the end, the user is also provided with the regime and the color of the regime where the pump's operating point is found. Additionally, the relative percentage error of the Q flow rate is presented, computed in relation to the measured flow rate value Q_{ms} if this variable has been included in the input data set. If the value of Q_{ms} was not mentioned in the input data set, then the relative percentage error of the flow rate will be missing.

We have used experimental data obtained for centrifugal pump PCN 65/200 at speed of $n = 2900$ rpm to validate the results supplied by the software. Preliminary validation of the software was performed at a speed of $n = 2500$ rpm. The data measured on the test rig available at the Hydraulic Machinery Laboratory of the "Politehnica" University Timişoara, presented in Figure 4, have been obtained using the IEC60193 methodology [33].

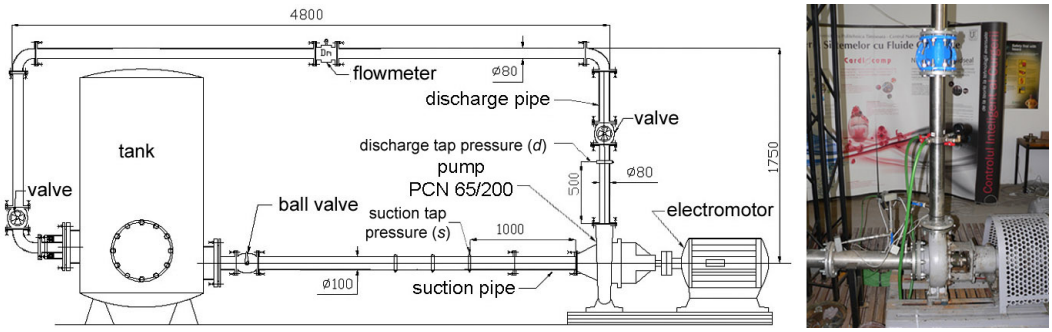

Figure 4. The test rig available at the Hydraulic Machinery Laboratory of the "Politehnica" University Timişoara. Schematic view of the test rig with actual dimensions in mm and photo.

A 22 kW asynchronous electrical motor is installed on the test rig to actuate the PCN 65/200 centrifugal pump. An ACS 850 45 kW Direct Torque Control (DTC) [34] inverter is used to vary the speed of the electrical motor from 500 rpm up to 3000 rpm [35]. A software platform completely controls the test rig. Firstly, an acquisition system was implemented to acquire sensor data for overall pressure, temperature, discharge, torque, speed and electrical power. The acquisition system with 32 input channels (voltage/current differential inputs) and a maximum 100 kb/s acquisition frequency was developed. The data is transferred to a computer using an RS232 interface. A remote control system was implemented, increasing

the operability of the test rig [36]. Next, a SCADA platform was implemented to acquire the needed variables (suction and discharge pressures, temperature, discharge, speed and torque) and store them in a log file.

The total uncertainty (f_t) is obtained by combining the uncertainties due to systematic (f_s) and random (f_r) errors. The systematic and random errors are evaluated taking into account the measuring system and the operating conditions of the pump (18).

$$f_t = \sqrt{(f_s)^2 + (f_r)^2} \tag{18}$$

The first step in the estimation of the pump efficiency uncertainty is to identify each component that can influence its value. As a result, the total uncertainty of the pump efficiency ($f_{t_{\eta_P}}$) of the discharge (f_{t_Q}), suction pressure ($f_{t_{p_s}}$), discharge pressure ($f_{t_{p_d}}$), speed (f_{t_n}) and torque (f_{t_T}) (19).

$$f_{t_{\eta_P}} = \sqrt{(f_{t_Q})^2 + (f_{t_{p_s}})^2 + (f_{t_{p_d}})^2 + (f_{t_n})^2 + (f_{t_T})^2} \tag{19}$$

The systematic errors are provided by the measuring devices. An electromagnetic flowmeter is used to measure discharge values up to 45×10^{-3} m^3/s with ±0.4% accuracy. This device is installed on the rig's top pipe. The suction pressure sensor range is –1 ÷ +2.5 bars with an accuracy of ±0.25%. The discharge pressure sensor range is 0 ÷ 6 bar with accuracy reported by the manufacturer of ±0.25%. A T22 torque transducer manufactured by HBM is installed on the test rig between the electrical motor and the centrifugal pump. The range from 0 to 100 Nm is covered by the torque transducer with an accuracy of ±0.5%. ROP520 incremental encoder is linked to the electrical motor shaft to measure the speed with an accuracy of ±0.01%. A systematic error of ±0.732% is obtained for the pump efficiency ($f_{s_{\eta_P}}$).

The random error is determined for the quantity acquired by each measuring device installed on the test rig using a set of ten values for ten operating points. As a result, the following maximum random errors are obtained for the measured quantities: the suction pressure of ±0.616%, the discharge pressure of ±0.658%, the discharge of ±0.18%, the speed of ±0.471% and the torque of ±0.387%. As a result, a random error value of ±1.103% is determined for the pump efficiency ($f_{r_{\eta_P}}$). Then, the total uncertainty of the pump efficiency ($f_{t_{\eta_P}}$) by ±1.323% is obtained on the test rig.

The ACS850 45 kW (DTC) inverter [34] is also used to acquire the electrical power, the mechanical power and the speed on the test rig. In this case, the total uncertainty for the mechanical power is determined using the accuracy of ±4% with nominal torque in an open loop and the speed control in a closed loop with an accuracy of 0.01% from the nominal speed. Then, the systematic error ($f_{s_{\eta_P}}$) of ±4.035% is obtained and the total uncertainty of ±4.183% for the pump efficiency ($f_{t_{\eta_P}}$). In conclusion, the total uncertainty of the pump efficiency is 3 times smaller if the torque transducer is installed on our test rig.

The software module was verified for the operation of the pump across its full operating range, covering all three operating regimes shown in Figure 5.

The curves $H = f(Q)$, $P_m = f(Q)$, and $\eta_P = f(Q)$ for the centrifugal pump PCN 65/200 at speed of $n = 2900$ rpm are shown in Figure 6. The experimental data are marked with dots, whilst the polynomial functions approximating them are plotted as continuous lines. These figures show a proper correlation between the experimental data and the approximation curves. The value of the R^2 parameter is shown for each curve, quantifying the accuracy of the approximation degree of the experimental data with the polynomial function selected in the software module.

Table 1 contains experimental data for centrifugal pump PCN 65/200. Tables 2–4 show the fitting coefficients for Equations (4), (10) and (11).

Table 1. The experimental data determined for centrifugal pump PCN 65/200 at speed of 2900 rpm.

OPno.	$Q_{ms} \times 10^3$ [m^3/s]	H_{ms} [m]	$P_{m_{ms}}$ [kW]	$\eta_{P_{ms}}$ [%]
OP7	6.727	49.678	11.815	27.737
OP8	12.289	48.861	13.497	43.629
OP9	18.640	47.295	15.816	54.662
OP10	24.232	45.104	17.109	62.645
OP11	29.604	42.387	18.145	67.818
OP12	33.668	38.439	18.827	67.411
OP13	37.213	36.266	18.888	70.070
OP14	40.037	33.721	19.110	69.282
OP15	42.560	31.468	18.939	69.348
OP16	44.617	28.774	18.781	67.036

Table 2. The coefficients of the 2nd-degree approximation polynomial function for the pumping head $H = f(Q)$ at speed of 2900 rpm.

n [rpm]	h_0	h_1	h_2	R^2
2900	49.859	105.330	−12,759.798	0.99791

Table 3. The coefficients of the 3rd-degree approximation polynomial function for the pump mechanical power $P_m = f(Q)$ at speed of 2900 rpm.

n [rpm]	p_0	p_1	p_2	p_3	R^2
2900	3.554	881.109	−13,978.015	40,315.701	0.96804

Table 4. The coefficients of the 2nd-degree approximation polynomial function for the pump efficiency $\eta_P = f(Q)$ at speed of 2900 rpm.

n [rpm]	e_0	e_1	e_2	R^2
2900	1.911	3834.803	−53,651.835	0.99599

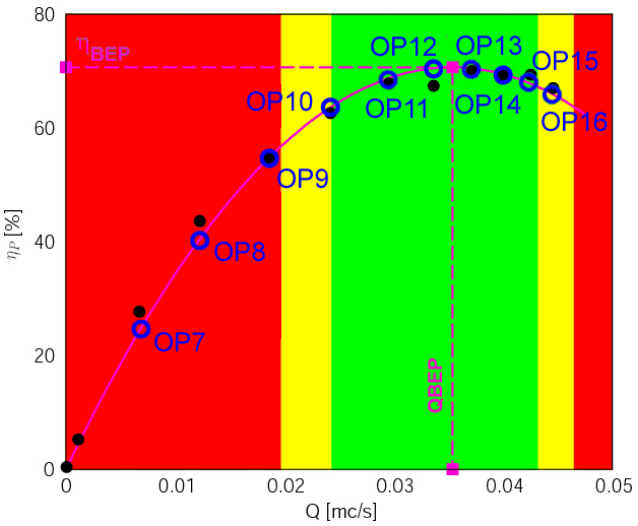

Figure 5. The validation of the software module for the pump's full operating range.

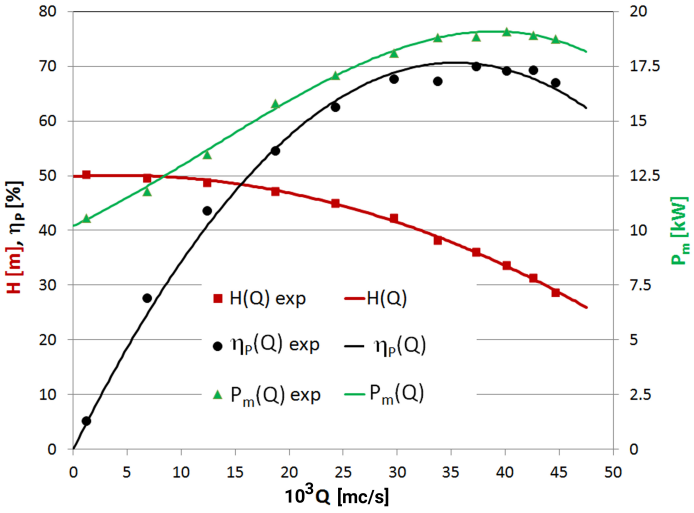

Figure 6. The experimental data for pumping head $H = f(Q)$ (■), mechanical power at the pump shaft $P_m = f(Q)$ (▲) and pump efficiency $\eta_P = f(Q)$ (●) at speed of 2900 rpm, together with polynomial curve fittings (solid lines).

The input parameters corresponding to the configuration of the test rig available at the "Politehnica" University Timişoara are as follows: the diameter of the suction line $D_s = 0.11$ m, the diameter of the discharge line $D_d = 0.08$ m, the position of the instrument on the suction line compared to the pump flange $l_s = 1.0$ m, the position of the instrument on the discharge line compared to the pump flange $l_d = 0.5$ m, the distributed hydraulic loss coefficient for the suction line $\lambda_s = 0.0158835$, the distributed hydraulic loss coefficient for the discharge line $\lambda_d = 0.0166889$, the local hydraulic loss coefficients for the suction and discharge lines $\zeta_s = \zeta_d = 0$ because no elbow was installed in the pump suction or discharge, the level difference between the position of the instrument on the discharge line and on the suction line $\Delta_z = 0.85$ m.

The last two columns in Table 5 ε_Q and ε_{η_P} are defined as $\varepsilon_\otimes$ in Equation (20):

$$\varepsilon_\otimes = \frac{\otimes_{ms} - \otimes}{\otimes_{ms}} 100[\%] \tag{20}$$

(corresponding to $y_i - f(x_i)$ in Equation (17)). $\eta_{P_{ms}}$ is the experimental data from Table 1, and η_P is the value calculated with curve fitting in Equation (11) with coefficients from Table 4. Q_{ms} is experimental read data in Table 1 and Q is calculated based on Equation (9).

The $\eta_{P_{ms}}$ experimental data in Table 1 are shown in Figures 5 and 7 with a black dot (●) and the calculated η_P values are shown with a white circle (○).

The input variables of each operating point are the static pressure measured at suction p_s [Pa], static pressure measured at discharge p_d [Pa] and optionally, the value of the measured volumetric flow rate Q_{ms} [m^3/s]. The following data are obtained for the pump speed of $n = 2900$ rpm: $H(\eta_{P_{BEP}}) = 37.33$ m, $P_m(\eta_{P_{BEP}}) = 17.19$ kW, $Q(\eta_{P_{BEP}}) = 35.7 \times 10^{-3}$ m^3/s.

See Figure 7a for operating point number 7 (*OP7*) set on partial flow rate during abnormal regime (AO). Our input values were: static pressure measured at suction $p_s = -9933.191$ Pa, static pressure measured at discharge $p_d = 47{,}0631.463$ Pa and the value of the volumetric flow rate measured by the flowmeter $Q_{ms} = 6.727 \times 10^{-3}$ m^3/s. The results provided by the software module for OP7 are: $Q = 6.35 \times 10^{-3}$ m^3/s, with a percentage error of -5.6% compared to $Q_{ms} = 6.727 \times 10^{-3}$ m^3/s, $\eta_P = 24.10\,\%$, $H = 50.01$ m, $P_m = 8.6$ kW. The abnormal operation diagnostic RED supplied is correctly determined.

Operating point number 9 (OP9) set on partial flow rate during abnormal regime (AO) (see Figure 7b) was checked with the following input values: static pressure measured at suction $p_s = -17{,}270.447$ Pa, static pressure measured at discharge $p_d = 435{,}108.521$ Pa and

the value of the volumetric flow rate measured by the flowmeter $Q_{ms} = 18.64 \times 10^{-3}\,\mathrm{m}^3/\mathrm{s}$. The results provided by the software module for OP9 are: $Q = 17.968 \times 10^{-3}\,\mathrm{m}^3/\mathrm{s}$, with a percentage error of -3.61% compared to $Q_{ms} = 18.64 \times 10^{-3}\,\mathrm{m}^3/\mathrm{s}$, $\eta_P = 53.49\,\%$, $H = 47.63\,\mathrm{m}$, $P_m = 15.1\,\mathrm{kW}$. The negative value of the percentage error shows that the flow rate value, determined by the software module, is lower than the value measured by the flowmeter. The abnormal operation diagnostic (AO) RED supplied is correctly determined.

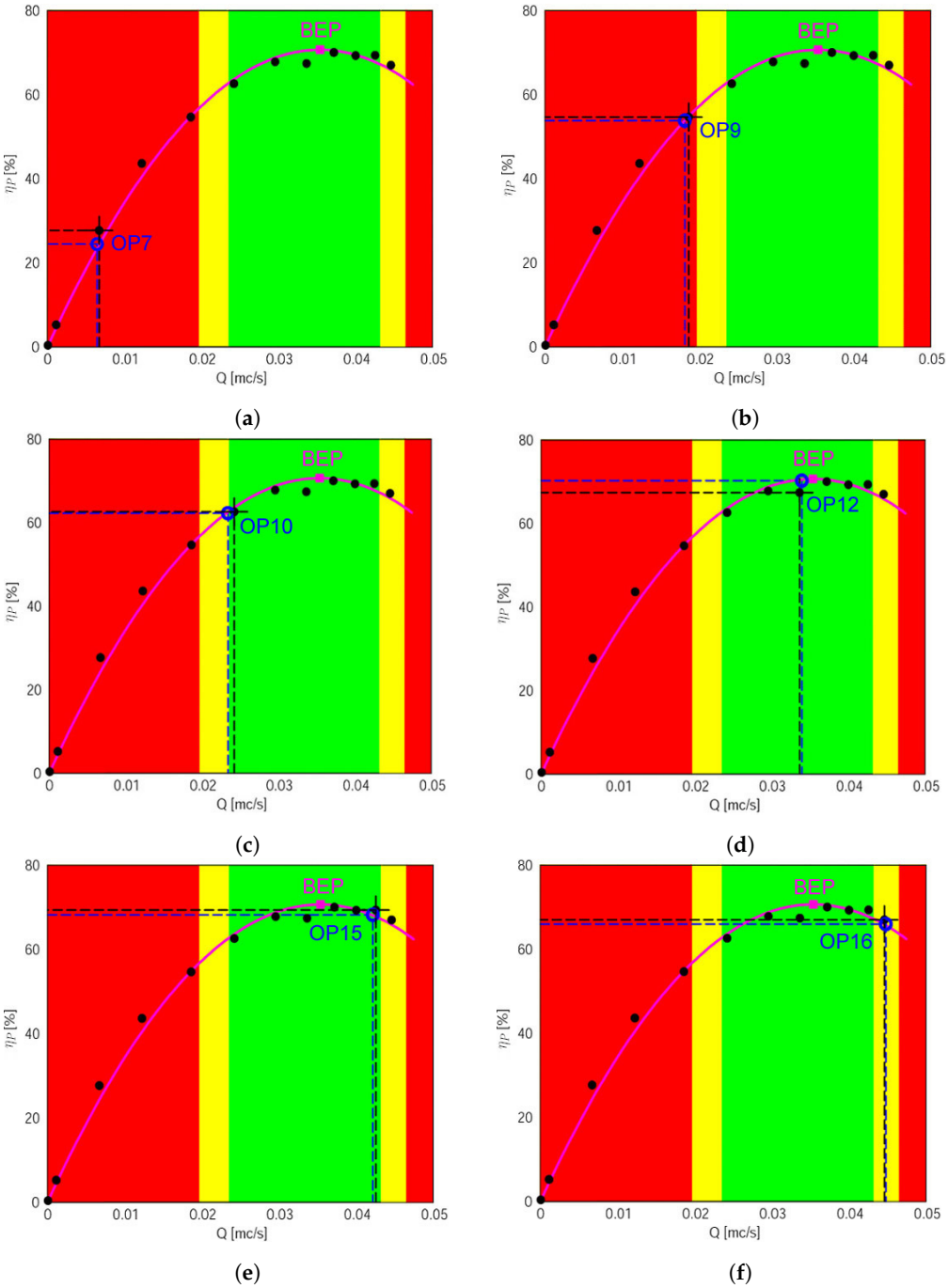

Figure 7. The validation of the algorithm for six operating points: (**a**) *OP*7: Q = $6.35\times10^{-3}\,\mathrm{m}^3/\mathrm{s}$, $\eta_P = 24.10\,\%$ (AO) RED; (**b**) *OP*9: Q = $17.968\times10^{-3}\,\mathrm{m}^3/\mathrm{s}$, $\eta_P = 53.49\,\%$ (AO) RED; (**c**) *OP*10: Q = $23.21\times10^{-3}\,\mathrm{m}^3/\mathrm{s}$, $\eta_P = 62.02\,\%$ (NO) GREEN (**d**) *OP*12: Q = $37.33\times10^{-3}\,\mathrm{m}^3/\mathrm{s}$, $\eta_P = 70.21\,\%$ (NO) GREEN (**e**) *OP*15: Q = $41.86\times10^{-3}\,\mathrm{m}^3/\mathrm{s}$, $\eta_P = 68.43\,\%$ (NO) GREEN (**f**) *OP*16: Q = $44.463\times10^{-3}\,\mathrm{m}^3/\mathrm{s}$, $\eta_P = 66.35\,\%$; (LO) YELLOW.

Table 5. The data computed by the software module for centrifugal pump PCN 65/200 at speed of 2900 rpm.

OPno.	$Q_{ms} \times 10^3$ [m^3/s]	H [m]	P_m [kW]	η_P [%]	ε_Q [%]	ε_{η_P} [%]
OP7	6.350	50.013	8.595	24.099	−5.602	13.114
OP8	12.321	49.220	12.363	41.014	0.257	5.993
OP9	17.968	47.632	15.106	53.494	−3.605	2.137
OP10	23.216	45.427	16.980	62.022	−4.191	0.994
OP11	29.691	41.738	18.447	68.473	0.295	−0.966
OP12	33.707	38.913	18.916	70.213	0.115	−4.157
OP13	37.792	35.616	19.065	70.208	1.555	−0.197
OP14	40.651	33.055	18.981	69.139	−1.647	0.206
OP15	41.859	31.911	18.901	68.425	−0.346	1.331
OP16	44.463	29.316	18.640	66.350	−0.346	1.023
BEP	35.738	37.327	17.190	70.435	—	—

The input variables for operating point number 10 (OP10) set on partial flow rate during normal regime (NO) (see Figure 7c) are: static pressure measured at suction $p_s = -18{,}530.6$ Pa, static pressure measured at discharge $p_d = 408{,}535.72$ Pa and the value of the volumetric flow rate measured by the flowmeter $Q_{ms} = 24.23 \times 10^{-3}$ m^3/s. The results provided by the software module for OP10 are: $Q = 23.21 \times 10^{-3}$ m^3/s, with a percentage error of −4.192% compared to $Q_{ms} = 24.23 \times 10^{-3}$ m^3/s, $\eta_P = 62.02$ %, $H = 45.427$ m, $P_m = 16.98$ kW. The normal operation diagnostic (NO) GREEN supplied is correctly determined.

The validation for the operating point number 12 (OP12) set in the vicinity of the maximum efficiency value during normal operation (NO) (see Figure 7d) shows the following input variables: static pressure measured at suction $p_s = -17{,}665.65$ Pa, static pressure measured at discharge $p_d = 335{,}325.2$ Pa and the value of the volumetric flow rate measured by the flowmeter $Q_{ms} = 33.67 \times 10^{-3}$ m^3/s. The results provided by the software module for OP12 are: $Q = 37.33 \times 10^{-3}$ m^3/s, with a percentage error of +0.113% compared to $Q_{ms} = 33.67 \times 10^{-3}$ m^3/s, $\eta_P = 70.21$ %, $H = 38.913$ m, $P_m = 18.96$ kW. The normal operation diagnostic (NO) GREEN supplied was predicted correctly.

The input variables for the operating point number 15 (OP15) set on overflow rate during normal regime (NO) (see Figure 7e) are: static pressure measured at suction $p_s = -27{,}807.4$ Pa, static pressure measured at discharge $p_d = 246{,}015.5$ Pa and the value of the volumetric flow rate measured by the flowmeter $10^3 Q_{ms} = 42.56$ m^3/s. The results provided by the software module for OP15 are: $Q = 41.86 \times 10^{-3}$ m^3/s, with a percentage error of −1.647% compared to $Q_{ms} = 42.56 \times 10^{-3}$ m^3/s, $\eta_P = 68.43$ %, $H = 31.911$ m, $P_m = 18.9$ kW. The normal operation diagnostic (NO) GREEN supplied is correctly identified.

The input variables for the operating point number 16 (OP16) set on overflow rate during normal regime (NO) (see Figure 7f) are: static pressure measured at suction $p_s = -29{,}996.15$ Pa, static pressure measured at discharge $p_d = 214{,}548.83$ Pa and the value of the volumetric flow rate measured by the flowmeter $Q_{ms} = 44.617 \times 10^{-3}$ m^3/s. The results provided by the software module for OP16 are: $Q = 44.463 \times 10^{-3}$ m^3/s, with a percentage error of −0.345% compared to $Q_{ms} = 44.617 \times 10^{-3}$ m^3/s, $\eta_P = 66.35$ %, $H = 29.316$ m, $P_m = 18.64$ kW. The operation at limit diagnostic (LO) YELLOW supplied is predicted correctly.

The analysis of the results supplied by the software module for the six operating points set on the full operating range of the pump shows the capacity of the software module to correctly identify the pump's operating regimes. The flow rate is a fundamental

hydraulic quantity that must be determined while the pump is in service. Determining the flow rate in situ is a challenge and a requirement for the water treatment technological process. The relative error of the flow rate estimated by the software module compared to the value measured by the flowmeter fits within the limit of −5.6% for the operating points with a flow rate below 25% of the value of the operating point with maximum efficiency. In exchange, the limit of the relative error is between −4.192% and +0.113% for all the operating points of the pump, except those with a flow rate below 25% of the value associated with the operating point with maximum efficiency. Based on the validated results, we can conclude that the software module allows estimating the flow rate of the pump's operating point when there is no flowmeter installed (or where there is no possibility to install one). The estimation of the flow rate using the software module is an additional gain to the assessment of the operating regime of the pump.

4.1. Sensitivity Analysis of the Algorithm for Various Operating Points

In some situations, particularly in situ, the input parameters in the software module cannot be precisely determined (e.g., the inner diameter of the line or the coefficient of longitudinal losses). This is why we have performed the sensitivity analysis of the output value (pump efficiency) in relation to the input values using the algorithm parameters. The variables that can influence the pump efficiency are: (1) input values read by the operator p_s [Pa] and p_d [Pa] and (2) the parameters of the algorithm corresponding to the in situ configuration, which are scanned from the unique barcode generated for each pump: (i) diameter of the line at suction/discharge $D_{s/d}$ [m]; (ii) the discharge transducer's quota compared to the suction transducer's quota $\Delta z_{d/s}$ [m]; (iii) the length of the line from suction/discharge up to the location of the pressure manometers (transducers) compared to the pump flanges $l_{s/d}$ [m]; and (iv) the coefficient of longitudinal losses along the suction/discharge line $\lambda_{s/d}$ [-].

To gain a more relevant view of how these parameters influence the pump's efficiency, the percentage variation of the pump efficiency has been represented in relation to the percentage variation of each input value. Moreover, to assess the sensitivity of the algorithm parameters for the pump's full range of operation, we have considered five operating points (OP8, OP9, OP10, OP12, OP14) from the range of flow rates corresponding to the defined areas (NO) GREEN, (LO) YELLOW, and (AO) RED on the efficiency curve.

In addition to the parameters used in the algorithm, for each configuration of a pump unit, the algorithm needs the input of the static pressure p_s, p_d read/recorded at the pump suction/discharge for each operating point. These values of the static pressure at the pump suction/discharge boast a great degree of erroneous readings. The error can come from the reading of analogical measurement tools, which are not all that accurate, or the reading of the values in the first part of the instrument scale, where there is a lower degree of accuracy. Errors can also come from the oscillation of these measurement instruments used in the operation of the pumps during transient or unsteady operating conditions.

The sensitivity analysis of the algorithm regarding the determination of the percentage deviation in the pump efficiency ϵ_{η_P} for the percentage static pressure variation ϵ_{p_d} for five operating points: OP8, OP9, OP10, OP12 and OP14 is shown in Figure 8. The percentage deviation of the pump efficiency ϵ_{η_P} is determined using Equation (21) where $\eta_P(\epsilon_x)$ is the value of the efficiency, determined for the percentage deviation of the input quantities (e.g., p_d, p_s, D_d, D_s, l_d, l_s, λ_d, λ_s, Δz).

$$\epsilon_{\eta_P} = \frac{\eta_P(\epsilon_x) - \eta_P}{\eta_P} 100 \ [\%] \tag{21}$$

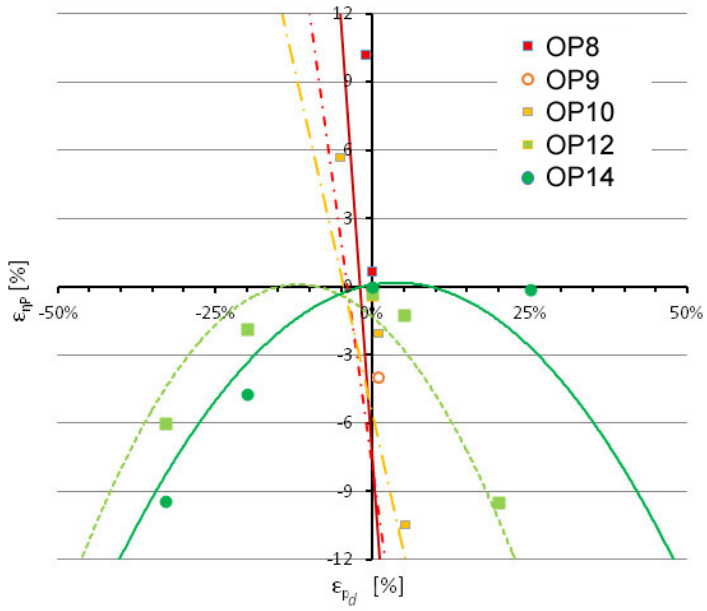

Figure 8. Sensitivity analysis of the algorithm regarding the determination of the pump efficiency ϵ_{η_P} for deviations in the reading of the discharge pressure ϵ_{p_d} for five operating points: OP8, OP9, OP10, OP12 and OP14.

One can notice the significant influence of the static pressure variation read at the pump discharge ϵ_{p_d} on the pump efficiency. The operating points laid out in the vicinity of the maximum efficiency influence the pump efficiency within the limit $\epsilon_{\eta_P} < \pm 12\%$ when the deviation of the static pressure determined at the pump discharge is read with a deviation within the limit $\epsilon_{p_d} < \pm 25\%$.

For the operating points laid out in the yellow and red zones, a slight deviation in the reading of the static pressure at the pump discharge $\epsilon_{p_d} > \pm 5\%$ leads to deviations in the values of the pump efficiency greater than $\epsilon_{\eta_P} > \pm 12\%$. For greater positive deviations at the reading of the static pressure at the pump discharge, an error message is returned because the input of the pressure difference between the pump suction and discharge is greater than the pumping head prescribed from the pump's catalog curve.

Figure 9 shows the algorithm sensitivity analysis for the determination of pump efficiency for the percentage variation of static pressure ϵ_{p_s} measured at the pump suction for the five operating points selected across the full range. One can notice a linear distribution of the pump efficiency variation, with the percentage variation of the static pressure ϵ_{p_s} measured at the pump suction. As expected, the variation of the static pressure read at the pump suction ϵ_{p_s} has a significant influence over the pump efficiency variation. The operating points located in the green area are an exception; the influence on the pump efficiency is less $\epsilon_{\eta_P} < \pm 1\%$ when the variation of the static pressure determined at pump suction is read with a deviation within the limit of $\epsilon_{p_s} < \pm 50\%$. Otherwise, for the operating points located in the yellow area, the pump variation can reach $\epsilon_{\eta_P} < \pm 5\%$ when the variation of the static pressure taken at pump suction is read with a deviation within the limit of $\epsilon_{p_s} < \pm 50\%$.

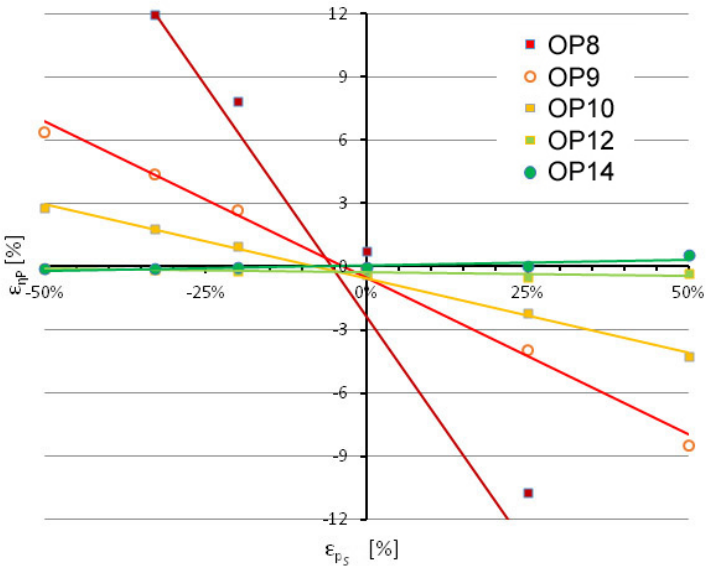

Figure 9. The algorithm sensitivity analysis regarding the determination of the pump efficiency ϵ_{η_P} for deviations in the reading of the suction pressure ϵ_{p_s} for five operating points: OP8, OP9, OP10, OP12 and OP14.

The algorithm sensitivity analysis for determining the pump efficiency for the variation of the line inner diameter at discharge ϵ_{D_d} for the five operating points across the operating range is shown in Figure 10. One can observe a significant variation of the pump efficiency ($\epsilon_{\eta_P} > \pm 3\%$) when we consider a deviation of the line inner diameter at discharge greater with $\epsilon_{D_d} > 25\%$ compared to its real value. The assessments for the two operating points located in the green area are an exception; the variation of the pump efficiency is below 3% ($\epsilon_{\eta_P} < -3\%$) even for a deviation of the line inner diameter at discharge greater up to $\epsilon_{D_d} < 50\%$ compared to its real value. For the situations where the exact value of the discharge line inner diameter D_d cannot be determined, it is preferable to consider a value higher than the real one.

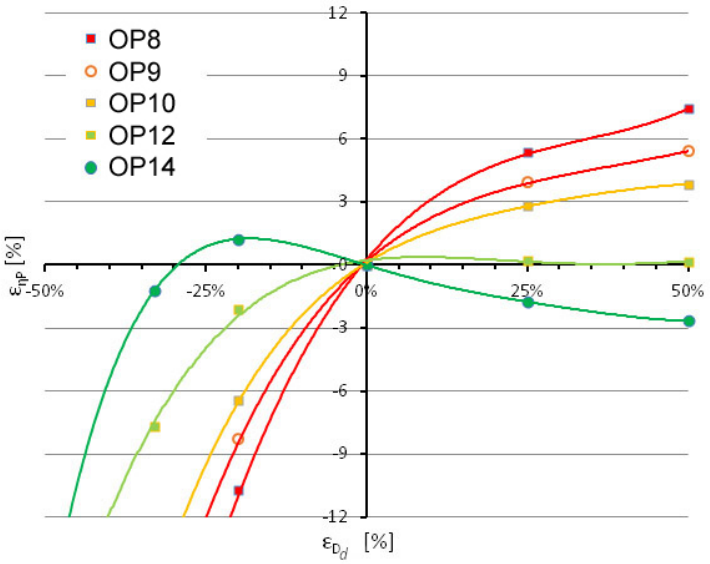

Figure 10. Algorithm sensitivity analysis regarding the determination of the pump efficiency ϵ_{η_P} or deviations in the input of the discharge line diameter ϵ_{D_d} for five operating points: OP8, OP9, OP10, OP12 and OP14.

Figure 11 shows the algorithm sensitivity analysis regarding the determination of pump efficiency for the variation of the suction line inner diameter ϵ_{D_s} for the five operating points across the full range. In Figure 11, one can notice a variation of the pump efficiency of up to 3% lower for the five operating points when the deviation of the suction pipe inner diameter is greater by up to $\epsilon_{D_s} < 50\%$ compared to its real value. In exchange, one can notice a significant variation of the pump efficiency ($\epsilon_{\eta_P} > \pm 5\%$) when it is considered a deviation of the suction line inner diameter below 33%, compared to its real value. An exception regarding the deviation of the suction line inner diameter is the situation where the assessment of the output is performed for the BEP. For the situations where the exact value of the suction line inner diameter D_s cannot be determined, it is preferable to consider a value higher than the real one. A reasonable approximation would be the outer diameter. In most cases, the approximation falls within the efficiency deviation $\epsilon_{\eta_P} < -3\%$.

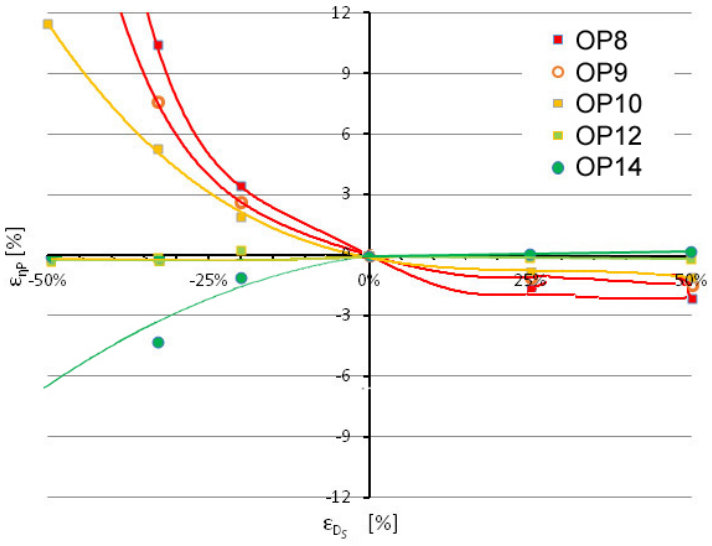

Figure 11. The algorithm sensitivity analysis for the determination of the pump efficiency ϵ_{η_P} for deviations in the input of the suction line diameter ϵ_{D_s} for the five operating points: OP8, OP9, OP10, OP12 and OP14.

If the suction and discharge diameters can be correctly measured on the outside, the inner values can be found in tables showing the thicknesses of the pipe wall. When establishing the inner diameters, it is preferable to consider a value that is greater than the real one. Another input parameter with an important influence on the efficiency algorithm is the variation of discharge pressure, Figure 8. The greatest deviations in the efficiency values are obtained at off-design conditions far away from the BEP corresponding to the maximum efficiency $\eta_{P_{BEP}}$.

The algorithm sensitivity analysis regarding the determination of the pump efficiency for the level variation between the two instruments that measure the suction/discharge pressure for the five operating points across the full range is shown in Figure 12.

One can notice a linear distribution of the pump efficiency variation with the deviation of the level $\epsilon_{\Delta z}$ defined in Equation (8) between the taps of the two instruments measuring the suction/discharge pressure compared to the reference value for the five operating points. As a result, a greater/smaller value of the pump efficiency is obtained when the deviation of the level $\epsilon_{\Delta z}$ is smaller or greater than the reference value. The pump efficiency value determined with the aid of the algorithm is within the limit of $\epsilon_{\eta_P} < \pm 1.5\%$ when the deviation of the level $\epsilon_{\Delta z}$ between the taps of the two instruments measuring the suction/discharge pressure deviate by $\epsilon_{\Delta z} < \pm 50\%$ compared to the reference value. The situations in which the operating points are laid out within the red area are an exception; the value of the pump efficiency determined with the algorithm is greater than $\epsilon_{\eta_P} > \pm 1.5\%$. The variation of the pump efficiency is more sensitive to the deviation of the inner diameters

of the suction/discharge lines $\epsilon_{D_s}/\epsilon_{D_d}$ than to the level deviation $\epsilon_{\Delta z}$ between the taps of the two instruments measuring the suction/discharge pressure.

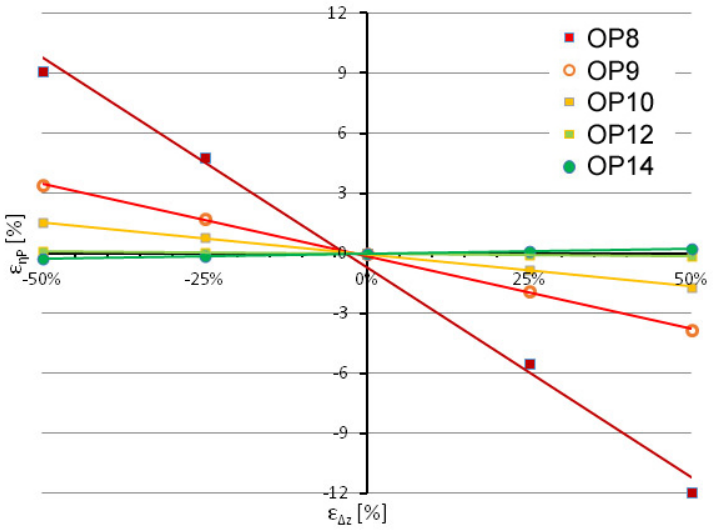

Figure 12. Algorithm sensitivity analysis regarding the determination of the pump efficiency ϵ_{η_P} for deviations in the input of the level difference $\epsilon_{\Delta z}$ between the locations of the transducers at suction and at discharge for the five operating points: OP8, OP9, OP10, OP12 and OP14.

Figure 13 shows the algorithm sensitivity analysis regarding the determination of pump efficiency for the variation of the layout position of the pressure tap length ϵ_{l_d} on the discharge line, compared to the pump's discharge flange for the five operating points across the full range. One would remark the fact that the variation of the layout position of the pressure tap length ϵ_{l_d} on the discharge line compared to the pump discharge flange has an insignificant influence on the pump efficiency variation $\epsilon_{\eta_P} < 1\%$ for all the operating points investigated.

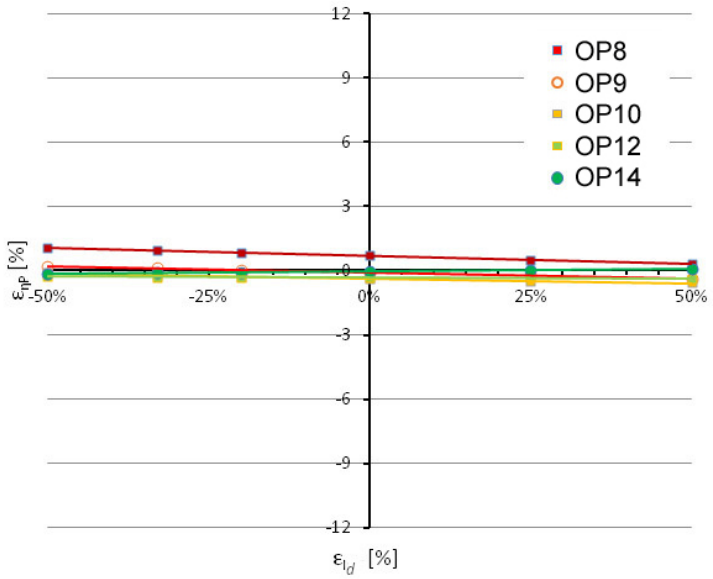

Figure 13. The algorithm sensitivity analysis regarding the determination of the pump efficiency ϵ_{η_P} for deviation in the length of the discharge line ϵ_{l_d} between the pressure transducer and the pump flange for the five operating points: OP8, OP9, OP10, OP12 and OP14.

Figure 14 shows the algorithm sensitivity analysis regarding the determination of the pump efficiency for the layout position of the pressure tap length ϵ_{l_s} on the suction line

compared to the pump's suction flange for the five operating points across the entire range. Note the same behavior of the algorithm regarding the variation of the pump efficiency $\epsilon_{\eta_P} < 1\%$ corresponding to the variation of the length ϵ_{l_s} for all the operating points assessed and for that of the length variation ϵ_{l_d}.

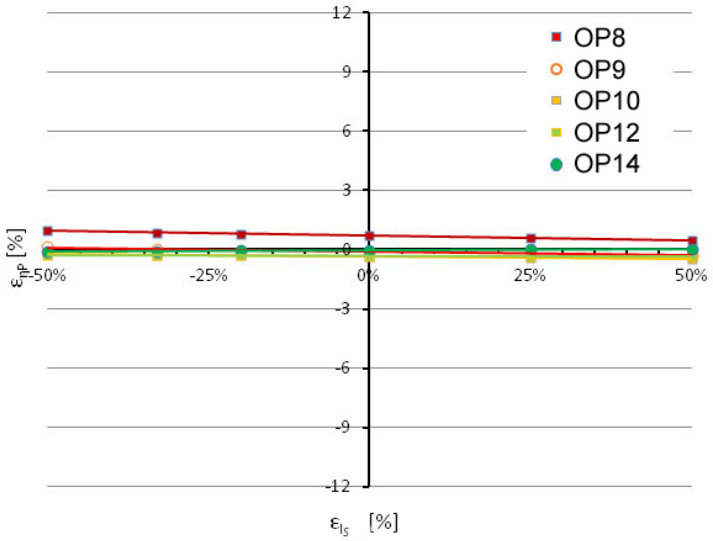

Figure 14. The algorithm sensitivity analysis regarding the determination of the pump efficiency ϵ_{η_P} or deviations in the length of the suction line ϵ_{l_s} between the pressure transducer and the pump flange for the five operating points: OP8, OP9, OP10, OP12 and OP14.

We can conclude that the influence of the layout positions of the pressure tap lengths ϵ_{l_s} and ϵ_{l_d} on the suction and discharge lines compared to the pump's suction and discharge flanges over the pump efficiency variation $\epsilon_{\eta_P} < 1\%$ is insignificant for the two operating points while functioning on a wider range.

Figures 15 and 16 show the algorithm sensitivity analysis regarding the determination of the pump efficiency for the variation of the hydraulic losses coefficient $\epsilon_{\lambda_d}/\epsilon_{\lambda_s}$ on the discharge/suction line, up to the layout position of the pressure tap, towards the pump's discharge/suction flange, for the five operating points across the entire operating range. The sensitivity of the algorithm regarding the determination of the pump efficiency for the variation of the hydraulic losses coefficient $\epsilon_{\lambda_d}/\epsilon_{\lambda_s}$ is identical to that produced by the length variation $\epsilon_{l_d}/\epsilon_{l_s}$. This situation is explained by the fact that the product of the two parameters $\epsilon_{\lambda_d}\epsilon_{l_d}/\epsilon_{\lambda_s}\epsilon_{l_s}$ are found in the equation of the pumping head. The influence of the hydraulic losses coefficient variation $\epsilon_{\lambda_d}/\epsilon_{\lambda_s}$ on the discharge/suction line up to the location of the pressure tap as opposed to the pump's discharge/suction flange over the pump efficiency variation $\epsilon_{\eta_P} < 1\%$ is insignificant for the five operating points across the entire range.

The results of the sensitivity analysis performed on the parameters used by the algorithm for the determination of the pump efficiency, implemented in the software module presented in this paper are summarized below. The parameters used in the algorithm are listed in the order of their importance on the pump efficiency:

- p_d [Pa]—static pressure at pump discharge;
- p_s [Pa]—static pressure at pump suction;
- D_d [m]—line diameter at discharge;
- D_s [m]—line diameter at suction;
- Δ_z [m]—transducer's level from discharge compared to that from suction;
- $l_{s/d}$ [m]—length of the suction/discharge line up until the location of the pressure manometers (transducers) compared to the pump flanges;
- $\lambda_{s/d}$ [-]—longitudinal hydraulic losses coefficient along the suction/discharge line;

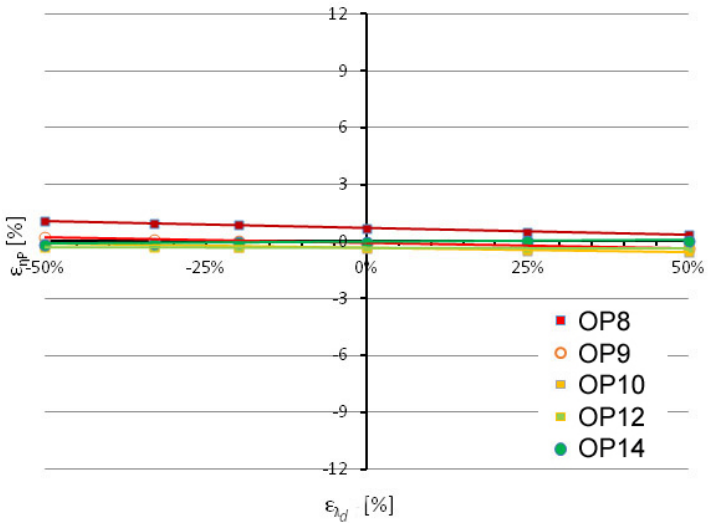

Figure 15. Algorithm sensitivity analysis regarding the determination of the pump efficiency ϵ_{η_P} for deviations in the input of the longitudinal losses coefficient for the discharge line ϵ_{λ_d} for the five operating points: OP8, OP9, OP10, OP12 and OP14.

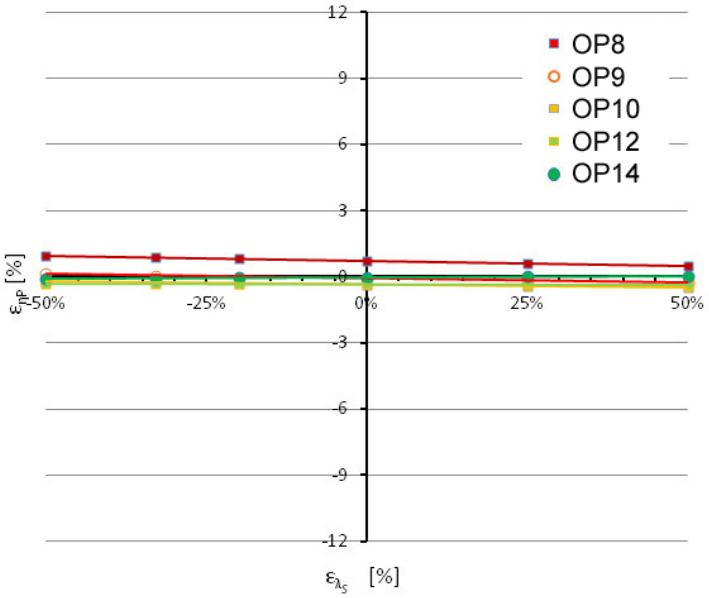

Figure 16. Algorithm sensitivity analysis regarding the determination of the pump efficiency ϵ_{η_P} or deviations in the input of the longitudinal losses coefficient for the suction line ϵ_{λ_s} for the five operating points: OP8, OP9, OP10, OP12 and OP14.

In conclusion, the determination of the input data that are characteristic to the pump, and the input of the read data, respectively, p_s and p_d, must be performed as accurately as possible to have the lowest influence on the pump efficiency η_P. It is recommended that the data acquired by the pressure transducers are taken directly into the software module to avoid any reading and data input errors.

The line diameter at discharge D_d has a greater influence on the pump's efficiency than the line diameter at suction D_s. This situation is because the centrifugal pumps tend to reach a higher pumping head, which is observed in a greater static pressure at discharge.

5. Assessment of a Pump's In Situ Operating Conditions Using the Software Module

The software module has been implemented at AQUATIM S.A. to monitor the operation of the double suction Worthington 500 LNN-775A double suction pumps of 1 MW, that supply Timişoara city with drinkable water.

The experimental data determined at the speed of 993 rpm by the manufacturer of the 1 MW double suction pump, installed at AQUATIM S.A., is listed in Table 6 and is marked with black dots (●) in Figure 17. Application of the algorithm presented in Section 2 has allowed the determination of the approximation polynomials' coefficients, which are shown in Table 7 for $H = f(Q)$, Table 8 for $P_m = f(Q)$ and Table 9 for $\eta_P = f(Q)$ and marked with continuous lines in Figure 17 of the polynomial functions approximating these experimental data. For the speed of 993 rpm, the $R^2 = 0.996$ parameter has had a value close to 1, indicating a good degree of approximation of the set of points with the selected polynomial function.

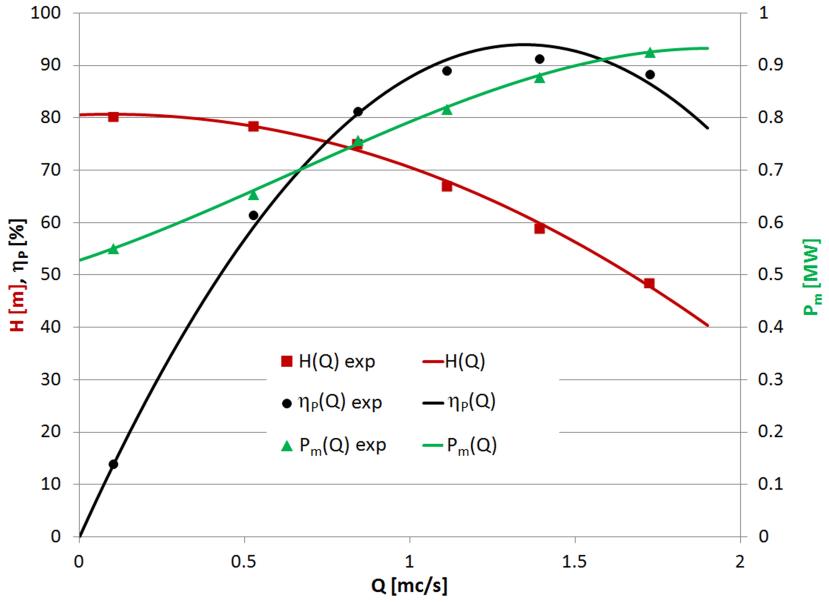

Figure 17. The experimental data provided by the manufacturer (■, ●, ▲) and the polynomial functions $H(Q)$, $P_m(Q)$ and $\eta_P(Q)$ determined for Worthington 500 LNN-775A double suction pump at speed of 993 rpm.

Table 6. The data for Worthington 500 LNN-775A double suction pump at speed of 993 rpm.

P no.	Q [m^3/s]	H [m]	P_m [MW]	η_P [%]
P1	0.0991	80.3	0.552	14.1
P2	0.5238	78.5	0.655	61.5
P3	0.8379	75.1	0.759	81.4
P4	1.1091	67.1	0.818	89.2
P5	1.3887	59.0	0.879	91.4
P6	1.7221	48.6	0.927	88.5
BEP	1.3498	61.189	0.874	93.804
DP	1.7191	48.071	0.926	86.860

Table 7. The coefficients of the 2nd-degree polynomial approximation function for the pumping head $H = f(Q)$ of the 1 MW Worthington pump at speed of 993 rpm.

n [rpm]	h_0	h_1	h_2	R^2
993	80.499	2.347	−12.338	0.995

Table 8. The coefficients of the 3rd-degree polynomial approximation function for the mechanical power $P_m = f(Q)$ of the 1 MW Worthington pump at speed of 993 rpm.

n [rpm]	p_0	p_1	p_2	p_3	R^2
993	0.528	0.209	0.113	−0.058	0.998

Table 9. The coefficients of the 2nd-degree polynomial approximation function for the efficiency $\eta_P = f(Q)$ of the 1 MW Worthington pump at speed of 993 rpm.

n [rpm]	e_0	e_1	e_2	R^2
993	1.056	137.427	−50.908	0.997

Figure 18 shows the curve of the pumping head ($H(Q)$) of the Worthington 500LNN-775A double suction pump of 1 MW, installed at AQUATIM S.A., at the speed of 993 rpm (continuous red line), determined based on the experimental data provided by the manufacturer. The curve for hydraulic losses ($H_r(Q)$) of the Timişoara city supply network (continuous blue line) is determined based on experimental data (♦ in Figure 18) obtained in situ. The duty point (DP, marked with a red circle (○) of this pump was determined to be at the intersection of the two curves $H(Q)$ and $H_r(Q)$.

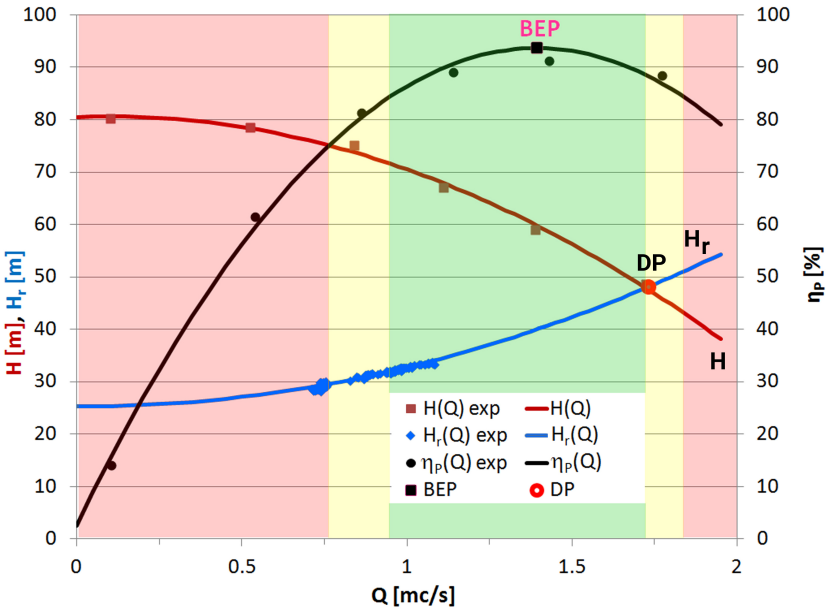

Figure 18. The duty point (DP) of a Worthington 500LNN-775A double suction pump of 1 MW at speed of 993 rpm operating in Timişoara drinking water network.

The input parameters for the Worthington 500 LNN-775A double suction pump of 1 MW, installed at AQUATIM S.A., read by the software module are: the suction line diameter $D_s = 0.6\,m$, and the discharge line diameter $D_d = 0.5\,$m. The instruments are installed on the pump flanges, meaning that $l_s = l_d = 0\,$m and the level difference between the location of the instruments installed on the discharge and suction flanges $\Delta z = 0.6\,$m. The hydraulic loss coefficients, distributed for the suction lines λ_s and discharge lines λ_d,

are not relevant in this case because the instruments are installed on the flanges, and the local hydraulic loss coefficients for the suction and discharge lines $\zeta_s = \zeta_d = 0$ because no elbow was installed in the pump suction or discharge. In this case, the pumping head is computed using the simplified formula presented in Equation (2) instead of the generalized formula presented in Equation (3).

The variable speed drive for Worthington 500 LNN-775A double suction pump includes an ACS 800-7 1000 kW DTC closed-loop speed inverter [37], but no torque transducer is installed in situ. This DTC inverter is manufactured by the same company as the one installed in the "Politehnica" University laboratory [34]. Both DTC inverters have the same torque and speed control performances [34,37]. In these conditions, the total uncertainty for the mechanical power is determined using the accuracy of ±4% with nominal torque in an open loop and the speed control in a closed loop with an accuracy of 0.01% from the nominal speed. As a result, a total uncertainty of over ±4% is predicted for the pump efficiency under in situ conditions.

The input data associated with pump performance over time have to be updated by the user. Certainly, the input data associated with pump performance have to be updated if repair work is applied to the geometry of the impeller blades. Assessing degraded pump performance in-service should be taken into account. Degraded pump performance methodology based on in-service test data is introduced by Gaiewski [38]. The methodology is based on the prediction of a small difference in the head at near pump shut-off head when compared to a new pump. An extensive degraded pump performance study on 150 pumps ranged from 22 kW to 3 MW installed in the municipal water supply and distribution system was conducted by Papa et al. [39]. The results obtained in this study revealed that the pump efficiency degraded by 9.3% on average when the pump operated at the BEP. Moreover, the efficiency degraded on average by 12.7% when the actual operating point and the original best efficiency point were compared. Papa et al. [39] noticed that while the ages of the pumps ranged from 1 year to 61 years with an average of 25 years, there was no discernible correlation between pump age and efficiency degradation. The above statement was not entirely surprising given that the pumps in service undergo various forms of routine maintenance, repair, refurbishment and modification throughout their working life [39].

The hydraulic performance along with the vibration response of an industrial scale centrifugal pump of 7.5 kW was experimentally investigated by [40,41] to assess the degradation in pump performance. The results delivered by all these investigations can be used to identify the degradation level in pump performance. As a result, the time when input data associated with pump performance has to be updated in the algorithm due to degradation is determined based on these investigations.

The marking of the $\eta_P(Q)$ curve for this pump allows the marking of the maximum efficiency value of $\eta_{P_{BEP}} = 93.6\,\%$ (marked with ■ in Figure 18) with a $+2.4\,\%$ deviation compared to the value indicated by the manufacturer, that of 91.4 %. The pump's operating regime (normal operation—NO, operation at limit—LO and abnormal operation—AO) have been determined according to the criteria defined in Section 2 and are marked by green, yellow and red.

The pump's duty point at a speed of 993 rpm can be found at the boundary between the green and the yellow areas (at a greater flow than that corresponding to the BEP flow rate). The selection of the pump's duty point for the maximum speed of 993 rpm is justified by the maximum flow rate of drinkable water supplied by this water treatment plant for Timişoara city. The operation of the pump in situ with VSD is considered to provide the variable flow rate needed by the consumers in Timişoara city.

6. Conclusions and Perspectives

This paper presents the development, implementation and validation of software developed for monitoring hydraulic pumps in service. The only parameter which is neither determined nor examined is the pump efficiency, although all the other variables (absorbed

power, pumping head) are measured to determine and calculate it. The goal of this software is to identify the hydraulic pumps' operating regimes in situ and to alert the user when they operate outside their preset efficiency range. The algorithm developed for assessing the efficiency of the hydraulic pump is based on knowing its features (available in the manufacturer's catalog or determined based on experimental investigations) and in situ geometric data. The input data of the algorithm are the geometric and hydraulic values related to the location of instruments compared to the position of suction/discharge flanges. The input data of each hydraulic pump installed in a station is unique, even though a station may use several identical pumps. The implemented algorithm provides the value of the pump efficiency η_P corresponding to the duty point. As a result, the operating regime is identified by collecting only the values of the suction p_s and discharge p_d static pressures. In addition to efficiency η_P, the algorithm delivers the following values for the duty point: pumping head H, the mechanical power at the pump shaft P_m, and the volumetric flow rate passed through the pump Q, which is a useful quantity in industrial applications but is difficult to determine in situ.

The algorithm is robust, and easy to use and implement, regardless of the user's training. The major advantage of the software, compared to other means of monitoring, is the easy in situ implementation because it does not require additional expenses. The pressure gauges are normally available at the suction and discharge of the hydraulic pump.

Free software packages have been selected for the algorithm to ensure its portability on any operating system. For example, the scientific software library GNU GSL provides robust interpolation, extrapolation and curve-fitting tools for the available data and for the assessment of the deviations. The free Qt package was selected for the graphic interface. The implementation of the algorithm is structured on independent components, materialized by individual procedures and tools in the command line, disconnected from the user interface. The data flow from the implemented software solution shown in the diagram in Section 3 provides a synoptic view of the processing and data transfer flow.

The software has been first used to analyze the operation of the centrifugal pump PCN 65/200, installed in the Hydraulic Pump Laboratory of the "Politehnica" University Timişoara. The research conducted on this pump was used to validate the output results delivered by the software module against experimental data over the full operating range. This software validation over the full operating range cannot be performed on pumps installed in situ due to the particular installing conditions and the limited operating range imposed on each pump. Moreover, the investigations carried out in the laboratory allowed the determination of the deviations of the results delivered by the software depending on the selected operating point over the full range of the pump. The analysis of the results delivered by the software for the six operating points laid out over the full pump range highlighted the capability to correctly identify the operating regime. The software module estimated the pump efficiency η_P within limits that do not affect the prediction of the operating regime.

We have previously stated that the volumetric flow rate is a fundamental hydraulic quantity that has to be determined while the pump is in service. This output quantity provided by the pump unit is directly related to the requirements of the process or system in which it operates. Therefore, the investigations conducted on the hydraulic pump installed in the laboratory have shown that the relative error of the volumetric flow rate estimated by the software module against the value measured by the flowmeter is up to -5.6% for the operating points with a flow rate below 25% of the value of the BEP. In exchange, the limit of the relative error is between -4.192% and $+0.113\%$ for all operating points, except those with a volumetric flow rate below 25% Q_{BEP}. The experimental data supports the conclusion that the software module allows estimating the flow rate of the operating point when there is no (or no possibility of installing) flowmeter installed. Estimating the volumetric flow rate using the software module is an additional gain on top of the assessment of the operating regime of the pump.

The sensitivity analysis of the input variables and parameters used in the algorithm highlighted their impact on the deviation of the output quantity (pump efficiency) and the operating point. The most significant impact on the efficiency deviation is provided by the pressure ($p_{d/s}$) values acquired at the discharge and the suction of the pump.

That is why the input data must be accurate enough to diminish the influence of the output value (e.g., the pump efficiency η_P). It is recommended that the data recorded by the pressure transducers are taken over directly to the software module to avoid any reading and data input errors. The impact of the discharge and suction pipe diameters ($D_{d/s}$) on the deviation efficiency is all the more significant when the selected values are smaller than the actual ones. Therefore, it is recommended that the outer diameters of the discharge and suction pipes be selected in the software module if it is not possible to measure the inner ones. In this case, the influence of the length ($l_{s/d}$) of the suction/discharge line between the pressure manometers (transducers) as well as the pump flanges and the longitudinal hydraulic losses coefficient ($\lambda_{s/d}$) along the suction/discharge line on the efficiency deviation are negligible. These input data can have a greater impact on the pump efficiency deviation if the measuring instruments are located at large distances from the pump and the pipelines have been in operation for a long time. The impact of the operating point on the pump efficiency deviation is all the greater the further we move away from the BEP.

The implementation of the software within the regional water supply company AQUATIM S.A. for monitoring in situ operations of pumps highlighted the demand for software products that can monitor high-efficiency pump operating regimes, justifying electricity costs according to European Union requirements, and supporting the predictive maintenance.

Note that the regional water supply company manages a fleet of hundreds of different hydraulic pumps, ranging from a few kilowatts to megawatts, that are distributed over a geographical area of hundreds of square kilometers. The development and implementation of software solutions to monitor the operation of the pump fleets are crucial in the management of the available resources in critical infrastructures.

The last section of the paper contains the results obtained with the software module for the Worthington 500 LLN-775A double-suction pump of 1 MW, which supplies drinkable water to the Timişoara city. The Worthington pumps are the most powerful pumps in the AQUATIM fleet and have been in service for 23 years. The pump's duty point at speed of 993 rpm is identified at the boundary between the green and the yellow region (at a greater flow rate than that corresponding to the BEP flow rate value). The choice of the pump's duty point for the maximum speed of 993 rpm is justified by the maximum flow rate of drinkable water supplied from this water treatment plant to Timişoara city.

In situ operation of the pumps with variable speed drive (VSD) is used to supply the variable flow rate needed by the consumers. The next stage in the development of the software consists of expanding its capabilities to monitor the efficiency of the VSD pumps. The work of this next stage is based on the obtained results and on the experience gathered to date.

Author Contributions: Conceptualization, A.-A.A. and S.M.; Data curation, A.-A.A., A.C. and S.M.; Funding acquisition, A.-A.A.; Investigation, A.-A.A. and S.M.; Methodology, A.-A.A. and S.M.; Project administration, A.-A.A.; Resources, A.C.; Software, A.-A.A.; Supervision, A.-A.A. and S.M.; Validation, A.-A.A., A.C. and S.M.; Visualization, A.-A.A. and S.M.; Writing-original draft, A.-A.A.; Writing-review & editing, A.-A.A. and S.M. All authors have read and agreed to the published version of the manuscript.

Funding: This research received no external funding

Institutional Review Board Statement: Not applicable.

Informed Consent Statement: Not applicable.

Data Availability Statement: Not applicable.

Acknowledgments: The authors acknowledge Eng. Daniel Moş for conducting experimental measurements on the PCN 65/200 pump. The author affiliated with "Politehnica" University Timişoara has been supported by the research contract BC27/27.03.2018 (https://staff.cs.upt.ro/~alin.anton/BC27/27.03.2018) (accessed on 7 November 2022). The author affiliated with Romanian Academy—Timişoara Branch has been supported by the research program of the Hydrodynamic and Cavitation Laboratory from the Center for Fundamental and Advanced Technical Research.

Conflicts of Interest: The authors declare no conflict of interest.

References

1. Pabi, S.; Amarnath, A.; Goldstein, R.; Reekie, L. *Electricity Use and Management in the Municipal Water Supply and Wastewater Industries*; Technical Report 3002001433; Water Research Foundation and Electric Power Research Institute: Palo Alto, CA, USA, 2013.
2. European Union Commission Regulation No 547/2012. Available online: https://data.europa.eu/eli/reg/2012/547/oj (accessed on 1 October 2022).
3. Sahoo, T.; Guharoy, A. Energy cost savings with centrifugal pumps. *World Pumps* **2009**, *2009*, 35–37. [CrossRef]
4. Bloch, H.P.; Budris, A.R. *Pump User'S Handbook: Life Extension*; River Publishers: New York, NY, USA, 2021.
5. EPRI. *Water and Wastewater Industries: Characteristics and Energy Management Opportunities*; Technical Report CR-106941; Electric Power Research Institute: Palo Alto, CA, USA, 1996.
6. Merkle, T. *Damages on Pumps and Systems: The Handbook for the Operation of Centrifugal Pumps*, 1st ed.; Elsevier: Oxford, UK, 2014.
7. Matlakala, M.; Kallon, D.; Simelane, S.; Mashinini, P. Impact of Design Parameters on the Performance of Centrifugal Pumps. *Procedia Manuf.* **2019**, *35*, 197–206. [CrossRef]
8. Guelich, J.F. *Centrifugal Pumps*, 1st ed.; Springer, Schmidt and Voeckler GbR: Leipzig, Germany, 2008.
9. Shiels, S. Centrifugal Pump Academy: Locating the greatest centrifugal pump energy savings. *World Pumps* **1998**, *1998*, 56–59. [CrossRef]
10. U.S. Environmental Protection Agency. *Fiscal year 2011: Drinking Water and Ground Water Statistics*; Technical Report EPA 816-R-13-003; U.S. Environmental Protection Agency, Office of Water: Washington, DC, USA, 2013.
11. KSB Guard Operating Manual. 2021. Available online: https://products.ksb.com/ (accessed on 1 October 2022).
12. de Almeida, A.T.; Fonseca, P.; Falkner, H.; Bertoldi, P. Market transformation of energy-efficient motor technologies in the EU. *Energy Policy* **2003**, *31*, 563–575. [CrossRef]
13. Ahonen, T.; Kortelainen, J.T.; Tamminen, J.K.; Ahola, J. Centrifugal pump operation monitoring with motor phase current measurement. *Int. J. Electr. Power Energy Syst.* **2012**, *42*, 188–195. [CrossRef]
14. Jussi Tamminen, T.A.; Ahola, J. Method and Arrangement for Estimating Flow Rate of Pump. U.S. Patent US9416787B2, 16 August 2016.
15. Ahonen, T. Monitoring of Centrifugal Pump Operation by a Frequency Converter. Ph.D. Thesis, LUT University, Lappeenranta, Finland, 2011.
16. Bertil Ohlsson, U.W.; Zahrai, S. Device, System and Method for On-Line Monitoring of Flow Quantities. U.S. Patent US6918307B2, 19 July 2005.
17. Gopalakrishnan, S.; Hanson, L. Pump with Integral Flow Monitoring. U.S. Patent US20030047008A1, 25 March 2003.
18. Sabini, E.P.; Lorenc, J.A. Centrifugal Pump Performance Degradation Detection. U.S. Patent US7112037B2, 26 September 2006.
19. Stuparu, A.; Baya, A.; Bosioc, A.; Anton, L.; Mos, D. Modelling the operation curves of two similar high power centrifugal pumps. *Am. Inst. Phys. Conf. Ser.* **2018**, *1978*, 030005. [CrossRef]
20. Stuparu, A.; Baya, A.; Bosioc, A.; Anton, L.; Mos, D. Experimental investigation of a pumping station from CET power plant Timisoara. *IOP Conf. Ser. Earth Environ. Sci.* **2019**, *240*, 032018. [CrossRef]
21. Brekke, H. A proposal for improving the thermodynamic method. In Proceedings of the 9th International Conference on Hydraulic Efficiency Measurements, Trondheim, Norway, 27–30 June 2012.
22. Carrasco, H.; Kengskool, K. Solutions to Industrial Engineering problems using integrated software environments. *Comput. Ind. Eng.* **1988**, *15*, 204–209. [CrossRef]
23. Wang, J.; Zhang, L.; Zheng, Y.; Wang, K. Adaptive prognosis of centrifugal pump under variable operating conditions. *Mech. Syst. Signal Process.* **2019**, *131*, 576–591. [CrossRef]
24. Johnson, H.A.; Simon, K.P.; Slocum, A.H. Data analytics and pump control in a wastewater treatment plant. *Appl. Energy* **2021**, *299*, 117289. [CrossRef]
25. Roozbeh Nia, A.; Awasthi, A.; Bhuiyan, N. Industry 4.0 and demand forecasting of the energy supply chain: A literature review. *Comput. Ind. Eng.* **2021**, *154*, 107128. [CrossRef]
26. Ferreira de Souza, D.; Antonio Marino Salotti, F.; Luis Sauer, I.; Tatizawa, H.; Gakiya Kanashiro, A. A Comparison Between Reported Values and Measured Values of Power Factor and Efficiency for Electric Induction Motors. *IEEE Lat. Am. Trans.* **2021**, *19*, 173–181. [CrossRef]
27. Takacs, G. *Electrical Submersible Pumps Manual: Design, Operations, and Maintenance*, 1st ed.; Gulf Professional Publishing: Oxford, UK, 2009.

28. Barringer, H. How to use reliability engineering principles for business issues. In Proceedings of the Proceedings, YPF Reliability Symposium, La Platta, Argentina, 30 November 1998.
29. Barringer, H.P.; Barringer & Associates, Inc. A life cycle cost summary. In Proceedings of the International Conference of Maintenance Societies, Mesa Perth, Australia, 20–23 May 2003 ; pp. 20–23.
30. Lai, Z.; Li, Q.; Zhao, A.; Zhou, W.; Xu, H.; Wu, D. Improving Reliability of Pumps in Parallel Pump Systems Using Particle Swam Optimization Approach. *IEEE Access* **2020**, *8*, 58427–58434. [CrossRef]
31. Galassi, M.; Davies, J.; Theiler, J.; Gough, B.; Jungman, G.; Alken, P.; Booth, M.; Rossi, F.; Ulerich, R. GNU Scientific Library Manual. Release 2.7, 2021. Available online: https://www.gnu.org/software/gsl/doc/latex/gsl-ref.pdf (accessed on 1 October 2022).
32. Qt Documentation. 2022. Available online: https://doc.qt.io/ (accessed on 1 October 2022).
33. *IEC 60193*; Hydraulic Turbines, Storage Pumps and Pump-Turbines—Model Acceptance Tests. International Electrotechnical Commission: Geneva, Switzerland, 2019.
34. *Low Voltage AC Drives ABB Machinery Drives ACS850 0.37 to 560 kW Catalog*; ABB Asea Brown Boveri Ltd.: Zurich, Switzerland, 2014.
35. Stanciu, R.; Ginga, G.; Muntean, S.; Anton, L. Low-speed-small-load direct torque control ripples filtering. *Proc. Rom. Acad. Ser. A Math. Phys. Tech. Sci. Inf. Sci.* **2012**, *13*, 125–132.
36. Stanciu, R.; Turcin, I.; Muntean, S.; Anton, L. Cellular wind-power integration using remotely controlled pump hydro energy storage. *Proc. Rom. Acad. Ser. A Math. Phys. Tech. Sci. Inf. Sci.* **2013**, *14*, 242–249.
37. *AC Drives ABB Machinery Drives ACS800*; Hardware Manual; ABB Asea Brown Boveri Ltd: Zurich, Switzerland, 2013.
38. Gaiewski, D. A Methodology for Determining Degraded Pump Performance Based on In-Service Test Criteria or Data. In Proceedings of the ASME 2011 Power Conference Collocated with JSME ICOPE 2011, Denver, CO, USA, 12–14 July 2011; Volume 2, pp. 255–259. [CrossRef]
39. Papa, F.; Radulj, D.; Karney, B.; Robertson, M. Pump energy efficiency field testing and benchmarking in Canada. *J. Water Supply Res. Technol.-Aqua* **2014**, *63*, 570–577. [CrossRef]
40. Eaton, A.; D'Alessandro, F.; Ahmed, W.; Hassan, H. On the Performance Degradation of Centrifugal Pumps. In Proceedings of the 5th International Conference of Fluid Flow, Heat and Mass Transfer (FFHMT'18), Niagara Falls, ON, Canada, 7–9 June 2018. [CrossRef]
41. Eaton, A.; Ahmed, W.H.; Hassan, M. Evaluating the Performance Degradation of Centrifugal Pumps Using the Principal Component Analysis. *J. Press. Vessel Technol.* **2021**, *144*, 021405. [CrossRef]